mRNA vaccine-induced SARS-CoV-2-specific T cells recognize B.1.1.7 and B.1.351 variants but differ in longevity and homing properties depending on prior infection status

Jason Neidleman[1, 2, †], Xiaoyu Luo[1, †], Matthew McGregor[1, 2], Guorui Xie[1, 2], Victoria Murray[3], Warner C. Greene[1, 4], Sulggi A. Lee[5, *], and Nadia R. Roan[1, 2, *, #]

[1] Gladstone Institute of Virology, San Francisco, CA, USA

[2] Department of Urology, University of California, San Francisco, CA, USA

[3] Zuckerberg San Francisco General Hospital and the University of California, San Francisco, CA, USA

[4] Departments of Medicine, and Microbiology and Immunology, University of California, San Francisco, CA, USA

[†]Equal contribution

[*]Co-correspondence:

nadia.roan@gladstone.ucsf.edu, sulggi.lee@ucsf.edu

[#]Lead contact

ABSTRACT

While mRNA vaccines are proving highly efficacious against SARS-CoV-2, it is important to determine how booster doses and prior infection influence the immune defense they elicit, and whether they protect against variants. Focusing on the T cell response, we conducted a longitudinal study of infection-naïve and COVID-19 convalescent donors before vaccination and after their first and second vaccine doses, using a high-parameter CyTOF analysis to phenotype their SARS-CoV-2-specific T cells. Vaccine-elicited spike-specific T cells responded similarly to stimulation by spike epitopes from the ancestral, B.1.1.7 and B.1.351 variant strains, both in terms of cell numbers and phenotypes. In infection-naïve individuals, the second dose boosted the quantity but not quality of the T cell response, while in convalescents the second dose helped neither. Spike-specific T cells from convalescent vaccinees differed strikingly from those of infection-naïve vaccinees, with phenotypic features suggesting superior long-term persistence and ability to home to the respiratory tract including the nasopharynx. These results provide reassurance that vaccine-elicited T cells respond robustly to the B.1.1.7 and B.1.351 variants, confirm that convalescents may not need a second vaccine dose, and suggest that vaccinated convalescents may have more persistent nasopharynx-homing SARS-CoV-2-specific T cells compared to their infection-naïve counterparts.

SUMMARY BULLET POINTS

- mRNA vaccine-elicited T cells respond identically to B.1.1.7 and B.1.351 spike
- Second mRNA dose affects quantity but not quality of vaccine-elicited T cells
- Convalescents' spike CD4 T cells express more CD127 and lung-homing receptors
- Spike CD4 T cell levels in blood inversely correlate with tissue migration markers

BRIEF SUMMARY

Neidleman et al. conducted CyTOF on antigen-specific T cells in longitudinal samples from infection-naïve and COVID-19 convalescent mRNA vaccinees. Vaccine-elicited T cells respond identically to variants, and change in quantity but not quality after first dose. Convalescents' T cells preferentially express the longevity-associated marker CD127 and respiratory tract homing receptors.

INTRODUCTION

Within 18 months of the December 2019 emergence of SARS-CoV-2, the novel betacoronavirus had already infected ~150 million people and taken the lives of over 3 million, nearly collapsed worldwide health systems, disrupted the global economy, and perturbed society and public health on a scale not experienced within the past 100 years. Fortunately, multiple highly-efficacious vaccines, including the two-dose mRNA-based ones developed by Pfizer/BioNTech and Moderna, which confer ~90% protection against disease, were approved for emergency use before the end of 2020. Although the vaccines provide the most promising route for a rapid exit from the COVID-19 pandemic, concerns remain regarding the durability of the immunity elicited by these vaccines and the extent to which they will protect against the variants of SARS-CoV-2 now spreading rapidly around the world.

The first variant observed to display a survival advantage was the D614G, which was more transmissible than the original strain and quickly became the dominant variant throughout the world (Korber et al., 2020). This variant, fortunately, did not evade immunity and in fact appeared to be more sensitive than the original strain to antibody neutralization by convalescent sera (Weissman et al., 2021). More worrisome, however, was the emergence at the end of 2020 of rapidly-spreading variants in multiple parts of the world, including B.1.1.7, B.1.351, P.1, and B.1.427/B.1.429 (originally identified in United Kingdom, South Africa, Brazil, and California, respectively) (Plante et al., 2021). Some variants, including B.1.1.7, may be more virulent (Davies et al., 2021). While antibodies against the original strain elicited by either vaccination or infection generally remain potent against B.1.1.7, their activity against B.1.351 and P.1 is compromised (Cele et al., 2021; Collier et al., 2021; Edara et al., 2021; Garcia-Beltran et al., 2021; Hoffmann et al., 2021; Kuzmina et al., 2021; Muik et al., 2021; Planas et al., 2021; Stamatatos et al., 2021; Wang et al., 2021). Antibodies from vaccinees were 14-fold less effective against B.1.351 than

against the ancestral strain, and a subset of individuals completely lacked neutralizing antibody activity against B.1.351 9 months or more after convalescence (Planas et al., 2021).

Reassuringly, early data suggest that relative to antibody responses, T cell-mediated immunity appears to be less prone to evasion by the variants (Redd et al., 2021; Skelly et al., 2021; Tarke et al., 2021). Among 280 CD4+ and 523 CD8+ T cell epitopes from the original SARS-CoV-2, an average of 91.5% (for CD4) and 98.1% (for CD8) mapped to regions not mutated in the B.1.1.7, B1.351, P.1, and B.1.427/B.1.429 variants. Focusing on just the spike response, the sole SARS-CoV-2 antigen in the mRNA-based vaccines, then 89.7% of the CD4+ epitopes and 96.4% of the CD8+ epitopes are conserved (Tarke et al., 2021). In line with this, the magnitude of the response of T cells from convalescent or vaccinated individuals was not markedly reduced when assessed against any of the variants (Tarke et al., 2021). The relative resistance of T cells against SARS-CoV-2 immune evasion is important in light of the critical role these immune effectors play during COVID-19. T cell numbers display a strong, inverse association with disease severity (Chen et al., 2020; Woodruff et al., 2020), and the frequency of SARS-CoV-2-specific T cells predicts recovery from severe disease (Neidleman et al., 2021; Rydyznski Moderbacher et al., 2020). SARS-CoV-2-specific T cells can also provide long-term, self-renewing immunological memory: these cells are detected more than half a year into convalescence, and can proliferate in response to homeostatic signals (Dan et al., 2021; Neidleman et al., 2020a). Furthermore, the ability of individuals with inborn deficiencies in B cell responses to recover from COVID-19 without intensive care suggests that the combination of T cells and innate immune mechanisms is sufficient for recovery when antibodies are lacking (Soresina et al., 2020).

Although T cells against the ancestral strain display a response of similar magnitude and breadth to the variants (Tarke et al., 2021), to what extent the variants change these T cells' phenotypes and effector functions is a different question. Small changes in the sequences of T cell epitopes, in the form of altered peptide ligands (APLs), can theoretically alter how the T cells respond to stimulation. Indeed, change of a single residue can convert a proliferative, IL4-

secreting effector response into one that continues to produce IL4 in the absence of proliferation (Evavold and Allen, 1991). Furthermore, APLs can activate Th1 cells without inducing either proliferation or cytokine production, shift Th1 responses into Th2-focused ones, and in some instances even render T cells anergic or immunoregulatory by eliciting TGFβ production (Sloan-Lancaster and Allen, 1996).

Another important aspect that hasn't been explored is to what extent vaccine- vs. infection-induced T cell responses differ phenotypically and funcitonally, and to what extent convalescent individuals benefit from vaccination as they already harbor some form of immunity against the virus. Studies based on the antibody and B cell response suggest that for COVID-19 convalescents, a single dose of the mRNA vaccines is helpful while the additional booster is not necessary (Ebinger et al., 2021; Goel et al., 2021; Stamatatos et al., 2021); how this translates in the context of vaccine-elicited T cell immunity is not clear.

To address these knowledge gaps, we conducted 39-parameter phenotyping by CyTOF on 24 longitudinal specimens from 8 mRNA-vaccinated individuals, 4 of whom had previously contracted and recovered from COVID-19. Blood specimens were obtained prior to vaccination, two weeks following the first dose, and two weeks following the second. For each individual, we assessed in depth the phenotypes and effector functions of total CD4+ and CD8+ T cells, and of CD4+ and CD8+ T cells responding to the original SARS-CoV-2 spike, to spike from variants B.1.1.7 and B.1.351, and to nucleocapsid. By conducting high-dimensional analyses on the resulting 120 datasets generated, we find a reassuringly unaltered T cell response against the variants, and a striking impact of prior infection on qualitative features of T cells elicited by vaccination.

RESULTS

Study Design

To characterize the phenotypic features of mRNA vaccination-elicited SARS-CoV-2-specific T cells, we procured 24 longitudinal blood samples from the COVID-19 Host Immune Response and Pathogenesis (CHIRP) cohort. Three of the participants had received the Moderna (mRNA-1273) vaccine, while the remaining five had received the Pfizer/BioNTech (BNT162b2) one. For all participants, longitudinal specimens were obtained at three timepoints: prior to vaccination, ~2 weeks (range 13-18 days) after the first vaccine dose, and ~2 weeks (range 6-28 days) after the second dose. Half of the participants were never infected with SARS-CoV-2, while the other half had completely recovered from mild (non-hospitalized) COVID-19 disease (Table S1). These prior infections had all occurred in the San Francisco Bay Area between March – July of 2020, when the dominant local strain was the original ancestral strain. Each specimen was phenotyped using a 39-parameter T cell-centric CyTOF panel (see Methods and Table S2) at baseline (to establish the overall phenotypes of total CD4+ and CD8+ T cells), and following 6 hours of stimulation with overlapping 15-mer peptides spanning the entire original (ancestral) SARS-CoV-2-spike, B.1.1.7 spike, B.1.351 spike, or the original SARS-CoV-2 nucleocapsid (the latter as a control for a SARS-CoV-2-specific response not boosted by vaccination). Including all the baseline and stimulation conditions, a total of 120 specimens from the 8 participants were analyzed by CyTOF.

SARS-CoV-2-specific T cells elicited by vaccination recognize B.1.1.7 and B.1.351 variants

We first confirmed our ability to identify SARS-CoV-2-specific T cells by stimulating PBMCs from vaccinated individuals with spike peptides. In line with our prior studies implementing a 6-hour peptide stimulation (Neidleman et al., 2020a; Neidleman et al., 2021), spike-specific CD4+ T cells could be specifically identified through intracellular cytokine staining for IFNγ, and a more robust response was observed among CD4+ than CD8+ T cells (Fig. 1A). Activation induced markers (AIM) such as Ox40, 4-1BB, and CD69 could also be identified in T

cells after spike peptide stimulation, but with a higher background in the baseline (no peptide stimulation) specimens relative to the intracellular cytokine staining approach (Fig. S1). For this reason, in this study we exclusively used IFNγ positivity in the peptide-stimulated samples as a marker of antigen-specific T cells.

In the infection-naïve participants, the first vaccination dose primed a spike-specific CD4+ T cell response, which was further boosted with the second dose (Fig. 1B, *top left*). For each participant and time point, the same number of cells were stimulated by exposure to the ancestral or variant spikes. This finding suggests that vaccine-elicited spike-specific CD4+ T cells recognize ancestral and variant spike equally well, and is consistent with their recently reported ability to recognize variant strains (Tarke et al., 2021). The response of vaccine-elicited CD8+ T cells to spike peptides was weaker, and mostly apparent only after the second dose (Fig. 1B, *top right*). As expected, vaccination did not elicit T cells able to respond to nucleocapsid peptides (Fig. 1C, *top panels*).

In contrast to the infection-naïve individuals where spike-specific CD4+ T cells were clearly elicited and then boosted upon the second dose, spike-specific CD4+ T cell responses in convalescent individuals did not show a consistent upward trend. Convalescent donor PID4112 had a large frequency of pre-vaccination SARS-CoV-2-specific CD4+ T cells that increased to >1% of the total CD4+ T cell frequency after the first dose and then dampened after dose 2 (Fig. 1B, *bottom left*). PID4112 also exhibited an elevated nucleocapsid-specific CD4+ T cell response after the first vaccination dose (Fig. 1C, *bottom left*), which may have been due to bystander effects resulting from the concomitant large spike-specific response. In comparison, PID4112's spike-specific CD8+ T cell response was low after dose 1, and boosted after dose 2 (Fig. 1B, *bottom right*). In contrast to PID4112, the remaining three convalescent donors exhibited an overall weak spike-specific T cell response. In fact, when comparing these three donors to the four infection-naïve donors, there was a highly significant decrease in the magnitude of the spike-specific CD4+ T cell response, while the spike-specific CD8+ T cell

response was equivalent between the two groups (Fig. 1D). These results were unexpected and suggest that, when excluding outlier PID4112, the magnitude of the vaccine-elicited spike-specific CD4+ T cell response was lower in convalescent individuals than in infection-naïve individuals.

These assessments of the magnitude of the spike-specific T cell response together suggest that 1) in infection-naïve individuals the CD4+ T cell response is boosted by the second vaccination dose, 2) convalescent individuals exhibit a more disparate response, with most donors mounting a weaker response than infection-naïve individuals, and 3) the response is more robust among CD4+ than CD8+ T cells. As a higher number of SARS-CoV-2-specific CD4+ T cells were available for analysis, we focused on this subset for our subsequent analyses.

Vaccine-elicited spike-specific CD4+ T cells responding to B.1.1.7 and B.1.351 spike are indistinguishable from those responding to ancestral spike

Leveraging our ability to not only assess the magnitude but also the detailed (39-parameter) phenotypic features of SARS-CoV-2-specific CD4+ T cells, we first determined whether the ancestral and variant spike epitopes stimulated different subsets of vaccine-elicited spike-specific CD4+ T cells. Such differences could theoretically result from the fact that ~5-10% of the spike epitopes differ between variants and ancestral strains (Tarke et al., 2021), and may therefore act as APLs steering responding cells towards different fates. We isolated the datasets corresponding to both post-vaccination timepoints for all eight donors, and then exported the data corresponding to spike-specific CD4+ T cells (as defined by IFNγ production, Fig. 1). After reducing the multidimensional single-cell data for each individual specimen to a two-dimensional datapoint through multidimensional scaling (MDS) (Ritchie et al., 2015), we observed the ancestral spike-stimulated samples to be interspersed among the B.1.1.7- and B.1.351-responding ones (Fig. 2A). We then visualized the spike-specific CD4+ T cells at the

single-cell level. When visualized alongside total (baseline) CD4+ T cells, spike-specific cells occupied a distinct “island” defined by high expression of IFNγ (Fig. 2B), suggesting unique phenotypic features of these cells. To better analyze these spike-responding CD4+ T cells, we visualized them in isolation within a new t-SNE which clearly demonstrated complete mixing of the cells stimulated by the ancestral, B.1.1.7, and B.1.351 spike proteins (Fig. 2C). Almost all of the responding cells expressed high levels of CD45RO and low levels of CD45RA (Fig. 2D), suggesting them to be memory cells. These memory CD4+ T cells included central memory T cells (Tcm), T follicular helper cells (Tfh), and those expressing multiple activation markers (CD38, HLADR, CD69, CD25) and receptors known to direct cells to tissues including the respiratory tract (CXCR4, CCR5, CCR6, CD49d) (Fig. 2E). The expression levels of these and all other antigens quantitated by CyTOF were not statistically different between CD4+ T cells responding to the three spike proteins (Fig. S2). To confirm the identical phenotypes of the three groups of spike-responding cells, we implemented unbiased clustering by flowSOM. Spike-stimulated cells were clustered into 8 subsets, and no subset was preferentially enriched in any one of the three groups (Fig. 2F). Together, these data suggest that vaccine-elicited spike-specific CD4+ T cells respond in the same manner to spike epitopes from the ancestral or variant strains, and would probably mount similar responses *in vivo* to infection by all three virus types.

The phenotypes of spike-specific CD4+ T cells do not change after the second vaccine dose

We next took advantage of our longitudinal study design to assess for any changes in the differentiation of spike-specific T cell responses over the course of the 2-dose vaccination. As the data presented above suggested no phenotypic differences between CD4+ T cells responding to the ancestral, B.1.1.7, and B.1.351 spike proteins, our subsequent analyses combined these datasets. We first assessed whether, among infection-naïve individuals, the

phenotypes of spike-specific CD4+ T cells were different after the first and second doses. Both MDS and tSNE visualizations of the data revealed that the cells from the two timepoints were interspersed, suggesting lack of phenotypic differences (Fig. S3A, B). This was confirmed by flowSOM clustering, which showed that although the first timepoint harbored fewer cells (Fig. S3C), it included the same flowSOM clusters as the second timepoint (Fig. S3D). Furthermore, no significant differences were observed in the frequencies of any of the clusters between the two timepoints (Fig. S3D). Manual gating revealed that the main canonical subsets of CD4+ T cells – the naïve (Tn), stem cell memory (Tscm), effector memory RA (Temra), central memory (Tcm), effector memory (Tem), T follicular helper (Tfh), and regulatory T cells (Treg) – did not differ significantly between the two timepoints. Interestingly, however, transitional memory T cell (Ttm) were higher at the later timepoint (Fig. S3F, G). Overall, Tcm and Tfh were the most abundant subsets among the spike-specific CD4+ T cells (Fig. S3F, G). These data together suggest that although the magnitude of the CD4+ T cell response is amplified by the second vaccine dose (Fig. 1B), its qualitative features are mostly unchanged by this booster.

We then conducted a similar analysis in the convalescent individuals. As the pre-vaccination timepoint included spike-specific CD4+ T cells primed by prior SARS-CoV-2 infection, we included all three timepoints in this analysis. When the data were visualized by MDS, it was apparent that most of the pre-vaccination specimens localized away from the post-vaccination specimens, which were interspersed with each other (Fig. 3A). Similar distinctions between pre-and post-vaccination specimens were visualized at the single-cell level by tSNE (Fig. 3B, C). Clustering of the cells by flowSOM revealed that although cells from each timepoint included all the clusters, the cluster distribution was markedly skewed among the pre-vaccination cells (Fig. 3D, E). Indeed, two clusters (C1, C3) were significantly over-represented and one (C5) under-represented among the pre-vaccination specimens (Fig. 3F). Interestingly, this altered distribution was not due to any changes in the main canonical subsets, which remained unaltered between the three timepoints (Fig. S4). To assess what may drive the

differences between the phenotypes of the pre- vs. post-vaccination spike-specific CD4+ T cells, we assessed for markers that were differentially expressed in clusters C1, C3, and C5. Interestingly, although clusters C1 and C3 were both over-represented among the pre-vaccination specimens, cluster C3 alone had diminished expression of multiple activation, co-stimulatory, and checkpoint inhibition markers (Fig. S5). These results suggest that the post-vaccination specimens may be enriched for spike-specific CD4+ T cells with higher levels of activation, co-stimulation, and checkpoint inhibition. Indeed, manual gating suggested that spike-specific CD4+ T cells that are activated (CD38+HLADR+), and express multiple co-stimulatory activating receptors (ICOS+Ox40+) or checkpoint molecules (PD1+CTLA4+) were significantly enriched among the post-vaccination specimens (Fig. 3G).

Together, these results suggest that, similar to the infection-naïve specimens, convalescent specimens exhibited no phenotypic differences between spike-specific CD4+ T cells after the first vs. second vaccination; however, there was a clear increase in the activation state of the infection-primed spike-specific CD4+ T cells even with the first vaccine dose that persisted after the second dose.

Vaccination-induced spike-specific CD4+ T cells from convalescent individuals exhibit unique phenotypic features of increased longevity and tissue homing

We next determined whether there were any phenotypic differences between the vaccine-induced spike-specific CD4+ T cells from the infection-naïve vs. convalescent individuals. Removal of convalescent outlier PID4112 revealed the magnitude of the spike-specific CD4+ T cell response to be lower in the convalescents than in infection-naïve participants after full vaccination (Fig. 1D). But when all donors were included there was no statistically significant difference in response magnitude (Fig. 4A). However, the spike-specific CD4+ T cells from the convalescent and infection-naïve individuals exhibited clear phenotypic differences when assessed by both MDS (Fig. 4B) and tSNE (Fig. 4C); this was most apparent

after the second vaccine dose, but could already be observed after the first. Since the cells after the second dose are more clinically relevant (as they are the ones persisting in vaccinated individuals moving forward), we focused our subsequent analysis on just this timepoint. When visualized as a dot plot, it was apparent that the spike-specific CD4+ T cells from infection-naïve individuals segregated away from those from the convalescents (Fig. 4D). Clustering of the data also demonstrated clear differences between the two patient groups (Fig. 4E, F), which was confirmed by demonstration of significant differences in cluster abundance (Fig. 4G).

To identify these phenotypic differences, we first assessed the relative distributions of the main canonical CD4+ T cell subsets. Interestingly, the vaccinated convalescents harbored significantly more spike-specific Tcm and less Ttm. There was also a trend ($p = 0.05$) for less Tem in these donors (Fig. 5A). In contrast, Tfh and Treg frequencies were not different between infection-naïve and convalescent vaccinees (Fig. 5B). To broaden our analysis, we assessed for unique features of cluster A1, which was over-represented in the infection-naïve donors, and cluster A3, which was over-represented in the convalescent donors (Fig. 4G). Interestingly, cluster A3 expressed high levels of CD127, CCR7, and CXCR4, while cluster A1 tended to express lower levels of these antigens (Fig. S6A). Confirming this finding, we also found that the expression levels of all three antigens were higher among the cells from the convalescent donors, although for CXCR4 the difference did not reach statistical significance (Fig. S6B).

We then followed up on each of these three differentially expressed markers. CD127, the alpha chain of the IL7 receptor, can drive IL7-mediated homeostatic proliferation of SARS-CoV-2-specific CD4+ T cells (Neidleman et al., 2020a), and serves as a marker of long-lived precursor memory cells (Kaech et al., 2003). To assess the potential longevity of the spike-specific CD4+ T cells, we determined the percentage of CD127+ cells expressing low levels of the terminal differentiation marker CD57. After the second dose of vaccination, convalescent individuals harbored more long-lived (CD127+CD57-) spike-specific CD4+ T cells than infection-naïve individuals (Fig. 5C). CCR7, the second preferentially-expressed marker among the

convalescents' spike-specific CD4+ T cells, is a chemokine receptor that directs immune cells to lymph nodes. As CD62L, a selectin that also mediates lymph node homing, was also on our panel, we assessed whether CCR7+CD62L+ cells were enriched among the spike-specific CD4+ T cells from the convalescent donors, and found this to be the case (Fig. 5D). The last differentially expressed antigen, CXCR4, was recently suggested to direct bystander T cells to the lung during COVID-19, and to be co-expressed with the T resident memory / activation marker CD69 (Neidleman et al., 2021). Interestingly, spike-specific CD4+ T cells from convalescent donors harbored a significantly higher proportion of CXCR4+CD69+ cells (Fig. 5E), suggesting a potentially superior ability to migrate into pulmonary tissues.

Our finding that the convalescent donors' spike-specific CD4+ T cells were preferentially CCR7+CD62L+ and CXCR4+CD69+ suggested that they may preferentially migrate out of the blood into tissues. Supporting this possibility was our observation that, after the second vaccine dose, the percentages of CCR7+CD62L+ and CXCR4+CD69+ spike-specific cells increased as the percentages of spike-specific CD4+ T cells decreased (Fig. 5F). This suggests that the low spike-specific CD4+ T cell response after the second dose of vaccination in some convalescent donors (Fig. 1D) may have resulted from these cells preferentially leaving the blood compartment. This was further supported by our finding that the expression levels of CCR7 and CD62L on spike-specific CD4+ T cells inversely correlated with the magnitude of the spike-specific CD4+ T cell response (Fig. 5G). To assess whether the CCR7+CD62L+ and CXCR4+CD69+ CD4+ T cells have the potential to migrate into the nasopharynx, the most common site of SARS-CoV-2 entry, we obtained paired blood and nasal swabs from one of the infection-naïve participants (PID4101) and phenotyped total CD4+ T cells isolated from these specimens. There was a marked enrichment of both CCR7+CD62L+ and CXCR4+CD69+ CD4+ T cells in the intranasal specimens (Fig. 5H), suggesting that CD4+ T cells expressing these markers preferentially exit the blood and enter the nasopharynx. Together, these data suggest that after vaccination, spike-specific CD4+ T cells from convalescent individuals differ from

those in infection-naïve individuals in that they appear to be more long-lived, and more readily migrate out of the blood to mucosal sites, thus explaining their overall lower frequencies measured from the blood.

Phenotypic differences of post-vaccination spike-specific CD4+ T cells are not due to different number of antigen exposures

The data presented above reveal striking phenotypic differences between spike-specific CD4+ T cells from convalescent vs. infection-naïve individuals after full vaccination. To try to understand the drivers of these differences, we assessed whether they could be accounted for by different numbers of antigen exposures. While the fully vaccinated infection-naïve donors were exposed twice to spike antigen, the fully vaccinated convalescent donors were exposed a total of three times. We first assessed whether the CCR7+CD62L+, CD57-CD127+, and CXCR4+CD69+ subsets that were more abundant in convalescent than infection-naïve donors after the second vaccine dose, were also more abundant after the first vs. second vaccine dose. We found they were not (Fig. 6A), arguing against the notion that three rounds of antigen exposure are necessary to elicit the unique phenotypes of spike-specific CD4+ T cells in convalescent vaccinees. We then compared these subsets between the infection-naïve donors after they had received both doses, vs convalescent donors after they received the first dose, with the rationale that both groups were exposed a total of two times to spike antigen. We found that all three subsets were significantly increased in the convalescent donors, and that the Tcm and Ttm subsets were also differentially present among the two groups (Fig. 6B). These results suggest that it is not the number of times one is exposed to antigen, but rather something intrinsic to prior infection, that drives the unique phenotypes of spike-specific CD4+ T cells in vaccinated, convalescent individuals.

Phenotypic features of spike-specific CD8+ T cells from vaccinated, convalescent individuals are unique but differ from their CD4+ T cell counterparts

Finally, we assessed to what extent the similarities and differences observed with spike-specific CD4+ T cells were also seen for spike-specific CD8+ T cells. Similar to the CD4+ T cells, spike-specific CD8+ T cells stimulated by the three different spike proteins (ancestral, B.1.1.7, B.1.351) did not differ in their phenotypic features (Fig. S7A-C). Also similar to the CD4+ T cells, spike-specific CD8+ T cells elicited by vaccination differed phenotypically in the infection-naïve vs. convalescent individuals (Fig. S7D-F). Unlike the CD4+ T cell data, however, these phenotypic differences could not be accounted for by distribution changes among the main canonical subsets Tn, Tscm, Temra, Tcm, Tem, and Ttm (Fig. S7G). Also unlike the CD4+ T cells, these differences were also not explained by differential abundance of the CD127+CD57-, CCR7+CD62L+, or CXCR4+CD69+ subsets (Fig. S7H). Instead, the differences appear to be due to other phenotypic changes, including elevated frequencies of activated cells in the convalescent donors, in particular those co-expressing the Tcm marker CD27 and activation marker CD38, and the checkpoint inhibitor molecule CTLA4 and activation marker 4-1BB (Fig. S7I). These results suggest that vaccine-elicited spike-specific CD8+ T cells, like their CD4+ counterparts, respond equivalently to the B.1.1.7 and B.1.351 variants, and exhibit qualitative differences in convalescent individuals but via different phenotypic alterations than their CD4+ counterparts.

DISCUSSION

T cells are important orchestrators and effectors during antiviral immunity. They may hold the key to long-term memory due to their ability to persist for decades, yet these cells have been disproportionately understudied relative to their humoral immune counterparts in the context of COVID-19. Here, we designed a longitudinal study assessing both the frequency and phenotypic characteristics of SARS-CoV-2-specific T cells in order to address the following

questions: 1) Do SARS-CoV-2-specific T cells elicited by vaccination respond similarly to ancestral and variant strains?, 2) To what extent is the second dose needed for boosting T cell responses in infection-naïve and convalescent individuals?, and 3) Do vaccine-elicited memory T cells differ in infection-naïve vs. convalescent individuals?

To answer the first question, we compared post-vaccination SARS-CoV-2 spike-specific T cell responses against ancestral vs. the variant B.1.1.7 and B.1.351 strains. Consistent with a recent study (Tarke et al., 2021), we find that vaccination-elicited T cells specific to the ancestral spike protein also recognize variant spike proteins. We further demonstrate that the phenotypic features of these cells are identical, whether they are stimulated by ancestral or variant spike proteins. This was important to establish because of prior reports that effector T cells can respond differently to APLs by altering their cytokine production or by mounting an immunoregulatory response (Evavold and Allen, 1991; Sloan-Lancaster and Allen, 1996). APLs could theoretically arise when a variant infects an individual that was previously exposed to ancestral spike through vaccination or prior infection. That both the quantity and quality of T cell responses is maintained against the variants may provide an explanation for the real-world efficacy of the vaccines against variants. Although limited data are available, thus far all vaccines deployed in areas where the B.1.1.7 or B.1.351 strains dominate have protected vaccinees from severe and fatal COVID-19 (Gupta, 2021). Given the potentially important role of SARS-CoV-2-specific T cells in protecting against severe and fatal COVID-19 (Dan et al., 2021; Neidleman et al., 2021), we postulate that this protection may have been in large part mediated by vaccine-elicited T cells. In contrast, efficacy of the vaccines against mild or moderate disease in variant-dominated regions of the world is more variable. For example, in South Africa where B.1.351 is dominant, the AstraZeneca ChAdOx1 vaccine only prevented ~10% of mild-to-moderate disease cases (Madhi et al., 2021), while more recent data from Pfizer/BioNTech's vaccine administered in Qatar, where both B.1.1.7 and B.1.351 are dominant, revealed that fully vaccinated individuals were 75% less likely to develop COVID-19 (Abu-

Raddad et al., 2021). The overall diminished vaccine-mediated protection against milder disease in variant-dominated regions of the world might be explained by the likely important role of antibodies to prevent initial infection by blocking viral entry into host cells (manifesting as protection against asymptomatic and mildly symptomatic infection), and the observation that vaccine-elicited antibodies are generally less effective against the variant than against ancestral spike in lab assays (Cele et al., 2021; Collier et al., 2021; Edara et al., 2021; Garcia-Beltran et al., 2021; Hoffmann et al., 2021; Kuzmina et al., 2021; Muik et al., 2021; Planas et al., 2021; Stamatatos et al., 2021; Wang et al., 2021). Reassuringly, there is no evidence that vaccinated individuals mount a weaker immune response to variants than do unvaccinated individuals, which could theoretically result through a phenomenon termed original antigenic sin (where the recall response is inappropriately diverted to the vaccination antigen at the expense of a protective response against the infecting variant strain) (Klenerman and Zinkernagel, 1998).

To address the second question of whether a booster dose is needed, we compared the T cells after the first vs. second vaccination doses, among the infection-naïve and convalescent individuals. In infection-naïve individuals, spike-specific responses were observed after the first vaccination dose, and were further boosted after the second. This enhancement of the T cell response after the second dose is similar to the reported increase in anti-spike IgG levels after a second dose in infection-naïve individuals (Ebinger et al., 2021; Goel et al., 2021). Interestingly, however, while the phenotypes of B cells producing the anti-spike antibodies differ after the first vs. second dose (converting from IgM-dominant to IgG-dominant B cells) (Goel et al., 2021), the phenotypes of the spike-specific CD4+ T cells between the two doses were remarkably similar. These cells were primarily Tcm and Tfh cells, the latter of which are important for providing helper function for B cells. The prominence of SARS-CoV-2-specific Tfh cells after just one dose of vaccination is consistent with prior reports that a single dose of SARS-CoV-2 mRNA in mice is sufficient to elicit potent B and Tfh cell responses in germinal centers (Lederer et al., 2020). These results suggest that with regards to T cells, the booster dose is necessary for enhancing

the magnitude but not quality of the response. Overall, however, our conclusions are in line with those drawn from serological studies (Ebinger et al., 2021; Goel et al., 2021): it is important to administer the second vaccine dose in infection-naïve individuals.

A different situation appears to be the case for convalescent individuals. Longitudinal serological studies suggest that the spike-specific antibody response in convalescent individuals after the first mRNA dose is already equivalent to that of infection-naïve individuals after their second mRNA dose (Ebinger et al., 2021; Goel et al., 2021), suggesting that convalescent individuals may only need a single dose of vaccination. We found no evidence of increased numbers of spike-specific CD4+ T cells after the second dose, and no phenotypic changes between the cells at the two timepoints. Spike-specific CD4+ T cells from these individuals did however exhibit marked phenotypic changes as they transitioned from the pre- to the post-vaccination timepoints. This was expected since the cells from the pre-vaccination timepoint are resting memory CD4+ T cells that were primed months prior, while the post-vaccination timepoints were more recently-reactivated memory cells. Interestingly, unlike for the infection-naïve individuals where all individuals responded similarly to each dose of vaccination, the magnitude of the CD4+ T cell response differed markedly between different convalescent individuals. PID4112 had a large pool of spike-specific CD4+ T cells prior to vaccination, and their numbers increased to extremely high levels after the first vaccination dose. Surprisingly, this large peak in the spike-specific response was accompanied by an increase in the nucleocapsid-specific CD4+ T cells, which was unexpected since the vaccine does not contain nucleocapsid. We suspect this high response to nucleocapsid was due to inflammation-mediated bystander activation of T cells in an antigen-independent manner. Consistent with this hypothesis, the participant reported severe side effects (severe headache, chills, myalgia, nausea, and diarrhea) after the first dose. The remaining three convalescent donors, by contrast, never exhibited a robust T cell response, and in fact after full vaccination actually exhibited a highly significantly lower CD4+ T cell response than the infection-naïve vaccinees.

We speculate on an explanation further below. Overall, our results suggest that a second SARS-CoV-2 vaccine dose in individuals who have recovered from COVID-19 may provide less benefit than in individuals who have not previously been exposed to SARS-CoV-2; these findings are in line with recommendations from previously published serological studies (Ebinger et al., 2021; Goel et al., 2021; Stamatatos et al., 2021).

One of the most striking observations from this study, and the third and final question we set out to answer, was the remarkably distinct phenotypes of spike-specific CD4+ T cells from infection-naïve vs. convalescent individuals who were fully vaccinated. These differences were not due to the additional round of antigen exposure experienced by the convalescent individuals, as they were already apparent in convalescent individuals after the first vaccine dose. The spike-specific CD4+ T cells from the convalescent individuals harbored features suggesting increased potential for long-term persistence: they were enriched for Tcm cells, which are have longer *in vivo* half-lives than their Tem and Ttm counterparts (Bacchus-Souffan et al., 2021), and express elevated levels of CD127, a marker of long-lived memory T cells (Kaech et al., 2003). Interestingly, CD127 expression on SARS-CoV-2-specific T cells has been implicated in COVID-19 disease amelioration and in these cells' long-term persistence. CD127 expression was more frequent on spike-specific CD4+ T cells from ICU patients who eventually survived severe COVID-19 than in those that did not (Neidleman et al., 2021). IL7, the ligand for CD127, can drive homeostatic proliferation and expansion of spike-specific CD4+ T cells (Neidleman et al., 2020a), and CD127 is not only expressed on SARS-CoV-2-specific memory CD4+ and CD8+ T cells, but its levels increase further over the course of convalescence (Ma et al., 2021; Neidleman et al., 2020a). Together, these findings suggest that after vaccination, spike-specific CD4+ T cells in convalescent individuals may persist longer than those from infection-naïve individuals, but additional long-term follow-up studies will be required to directly test whether this indeed is the case.

Another interesting characteristic of post-vaccination spike-specific CD4+ T cells from convalescent individuals relative to infection-naïve individuals was their expression of multiple tissue-homing receptors. In particular, these cells were preferentially CCR7+CD62L+ and CXCR4+CD69+. CCR7 and CD62L mediate homing to lymph nodes, while CXCR4 is a chemokine receptor important in migration of hematopoietic stem cells to bone marrow, but also able to direct immune cells to the lung during inflammation (Mamazhakypov et al., 2019). Interestingly, we recently observed co-expression of CXCR4 with CD69 (an activation marker that also identifies T resident memory cells) in pulmonary T cells from COVID-19 patients (Neidleman et al., 2021). Many of these cells were bystander (non-SARS-CoV-2-specific) CXCR4+CD69+ T cells whose numbers in blood increased prior to death from COVID-19. We therefore proposed a model whereby recruitment of non-SARS-CoV-2-specific T cells into the lungs of severe patients may exacerbate the cytokine storm and thereby contribute to death (Neidleman et al., 2021). In the case of the vaccinated convalescent individuals, however, expression of CXCR4 and CD69 on SARS-CoV-2-specific T cells is expected to be beneficial as it would direct the T cells capable of recognizing infected cells into the lung. CCR7 and CD62L co-expression would further enable these cells to enter draining lymph nodes and participate in germinal center reactions. Supporting the hypothesis that the post-vaccination spike-specific CD4+ T cells from convalescent individuals may better home to the respiratory tract is our observation that frequencies of these cells in blood correlated negatively with the extent to which they co-expressed CCR7 and CD62L, and to a lesser extent CXCR4 and CD69. This was further supported by our finding that CD4+ T cells from the nasopharynx of the upper respiratory tract were preferentially CCR7+CD62L+ and CXCR4+CD69+ relative to their blood counterparts. All together, these results imply that compared to infection-naïve individuals, convalescents' spike-specific CD4+ T cells may be superior in surviving and migrating to the respiratory tract. Directly testing this hypothesis will require obtaining large numbers of respiratory tract cells from vaccinated, infection-naïve vs. convalescent individuals (e.g., via

bronchoalveolar lavages or endotracheal aspirates) for quantitation and characterization of SARS-CoV-2-specific T cells. Of note, vaccination of infection-naïve individuals might not induce a strong humoral immunity in the respiratory mucosa either, as neutralizing antibodies against SARS-CoV-2 are rarely detected in nasal swabs from vaccinees (Planas et al., 2021). If it turns out that current vaccination strategies do not ensure robust humoral and cell-mediated immune responses in the respiratory tract, then strategies that better elicit mucosal-homing SARS-CoV-2-specific B and T cells in infection-naïve individuals – for example by implementing an intranasal route of mRNA immunization – may hold a greater chance of achieving sterilizing immunity.

Limitations

As this study was aimed at using in-depth phenotypic characterization as a discovery tool, it focused on deeply interrogating many different conditions (e.g., spike variants, longitudinal sampling) rather than many donors. Therefore, although a total of 120 CyTOF specimens were run, only 8 donors were analyzed. The findings reported here should be confirmed in larger cohorts. A second limitation of the study was the need to stimulate the specimens in order to identify and characterize the vaccine-elicited T cells. We limited peptide exposure to 6 hours to minimize phenotypic changes caused by the stimulation. We note that at this time, stimulation with peptides is the only way to identify SARS-CoV-2-specific CD4+ T cells as robust MHC class II multimer reagents for SARS-CoV-2 are not available currently. Finally, the analysis focused on CD4+ T cells because the overall numbers of detectable spike-specific CD8+ T cells were low. Nonetheless, the main findings we made with the CD4+ T cells – that they recognize variants equivalently, and that the phenotypes of the responding cells differ by prior SARS-CoV-2 natural infection status – were recapitulated among CD8+ T cells. Additional studies in a larger number of participants testing more cells, and implementing the use of MHC class I

tetramers, would increase the ability to characterize in greater depth the vaccine-elicited CD8+ T cell response.

ACKNOWLEDGEMENTS

This work was supported by the Van Auken Private Foundation, David Henke, and Pamela and Edward Taft (N.R.R.); philanthropic funds donated to Gladstone Institutes by The Roddenberry Foundation and individual donors devoted to COVID-19 research (N.R.R.); the Program for Breakthrough Biomedical Research (N.R.R., S.A.L.), which is partly funded by the Sandler Foundation; and Awards #2164 (N.R.R.), #2208 (N.R.R.), and #2160 (to S.A.L.) from Fast Grants, a part of Emergent Ventures at the Mercatus Center, George Mason University. We acknowledge the NIH DRC Center Grant P30 DK063720 and the S10 1S10OD018040-01 for use of the CyTOF instrument. We thank Stanley Tamaki and Claudia Bispo for CyTOF assistance at the Parnassus Flow Core, Heather Hartig for help with recruitment, Françoise Chanut for editorial assistance, and Robin Givens for administrative assistance.

AUTHOR CONTRIBUTIONS

J.N. designed and performed experiments, and conducted data analyses; X.L. helped develop an analysis plan and conducted data analyses; M.M. processed and banked specimens; G.X. performed experiments; V.M. conducted CHIRP participant interviews, enrollment, and specimen collection; W.C.G. participated in data analysis, performed supervision, and edited the manuscript; S.A.L. established the CHIRP cohort, conducted CHIRP participant interviews, enrollment, and specimen collection, and edited the manuscript; N.R.R. conceived ideas for the study, performed supervision, conducted data analyses, and wrote the manuscript. All authors read and approved the manuscript.

COMPETING FINANCIAL INTERESTS: The authors declare no competing financial interests.

METHODS

RESOURCE AVAILABILITY

Lead Contact

Requests for resources and reagents and for further information should be directed to and will be fulfilled by the Lead Contact, Nadia Roan (nadia.roan@gladstone.ucsf.edu).

Materials Availability

This study did not generate new unique reagents.

Data and Code Availability

For this study, a total of 120 specimens were analyzed by CyTOF. Each specimen included both CD4+ and CD8+ T cells. For each specimen, we gated separately on events corresponding to CD4+ T cells (live, singlet CD3+CD4+CD8-) and CD8+ T cells (live, singlet CD3+CD4-CD8+), and exported the files as 240 individual FCS files. These 240 raw CyTOF datasets are available for download through the public repository Dryad via the following link: https://doi.org/10.7272/Q60R9MMK

EXPERIMENTAL MODEL AND SUBJECT DETAILS

Human Subjects

Eight participants from the COVID-19 Host Immune Pathogenesis (CHIRP) cohort were recruited for this study. Four were previously infected with SARS-CoV-2 as established by RT-PCR, and had fully recovered from a mild course of disease. Importantly, infections of these four individuals had all occurred in the San Francisco Bay Area between March – July of 2020, when the dominant local strain was the original ancestral (Wuhan) strain. The remaining four participants were not previously infected with the virus. All eight participants were vaccinated with both doses of either of the Moderna or Pfizer/BioNTech mRNA vaccines (Table S1). Blood was drawn from each of the 8 participants prior to vaccination, ~2 weeks after the first vaccine

dose, and ~2 weeks after the second vaccine dose (24 specimens total). On the day of each blood draw, PBMCs were isolated from blood using Lymphoprep™ (StemCell Technologies), and then cryopreserved in 90% fetal bovine serum (FBS) and 10% DMSO. For participant PID4101, an additional blood-draw and intranasal swab specimens were obtained for immunophenotyping studies. This study was approved by the University of California, San Francisco (IRB # 20-30588).

METHOD DETAILS

Preparation of specimens for CyTOF

Cryopreserved PBMCs were revived and cultured overnight to allow for antigen recovery. The cells were then counted, and then two million cells per treatment condition were stimulated with the co-stimulatory agents 0.5 μg/ml anti-CD49d clone L25 and 0.5 μg/ml anti-CD28 clone L293 (both from BD Biosciences), in the presence of 0.5 μM of overlapping 15-mer SARS-CoV-2 spike peptides PepMix™ SARS-CoV-2 peptides from the original SARS-CoV-2 strain, B.1.1.7, or B.1.351, or overlapping 15-mer SARS-CoV-2 nucleocapsid peptides (all from JPT Peptide Technologies). Stimulations were conducted for 6 hours in RP10 media (RPMI 1640 medium (Corning) supplemented with 10% FBS (VWR), 1% penicillin (Gibco), and 1% streptomycin (Gibco)), in the presence of 3 μg/ml Brefeldin A Solution (eBioscience) to enable detection of intracellular cytokines. To establish the phenotypes of total T cells in the absence of stimulation, two million cells were cultured in parallel with the stimulated samples, but in the presence of only 3 μg/ml Brefeldin A.

After culture, the cells were treated with cisplatin (Sigma-Aldrich) as a live/dead marker and fixed with paraformaldehyde (PFA) as previously described (Ma et al., 2020; Neidleman et al., 2020a). Cisplatin treatment and fixation was performed as follows: first, cells were resuspended in 2 ml PBS (Rockland) with 2 ml EDTA (Corning), followed by addition of 2 ml

PBS/EDTA supplemented with 25 μM cisplatin (Sigma-Aldrich) for 60 seconds. Cisplatin staining was then quenched with 10 ml of CyFACS (metal contaminant-free PBS (Rockland) supplemented with 0.1% FBS and 0.1% sodium azide (Sigma-Aldrich)), centrifuged, and resuspended in 2% PFA in CyFACS. Fixation was allowed to proceed for 10 minutes at room temperature, after which cells were washed twice with CyFACS, and then resuspended in CyFACS containing 10% DMSO. Fixed cells were stored at -80°C until analysis by CyTOF. For paired blood/swab specimens from PID4101, cells were immediately cisplatin-treated and fixed, without prior cryopreservation.

CyTOF staining and data acquisition

CyTOF staining was conducted in a fashion similar to recently described methods (Cavrois et al., 2017; Ma et al., 2020; Neidleman et al., 2020a; Neidleman et al., 2020b; Neidleman et al., 2021; Xie et al., 2021). Cisplatin-treated cells were thawed, counted, and each treatment condition was barcoded using the Cell-ID 20-Plex Pd Barcoding Kit (Fluidigm). After the cells were barcoded and washed, the barcoded samples were combined and diluted to 6 x 10^6 cells / 800 μl CyFACS per well in Nunc 96 DeepWell™ polystyrene plates (Thermo Fisher). Cells were blocked with mouse (Thermo Fisher), rat (Thermo Fisher), and human AB (Sigma-Aldrich) sera for 15 minutes at 4°C, and then washed twice in CyFACS. Surface CyTOF antibody staining (Table S2) was conducted for 45 minutes at 4°C, in a volume of 100 μl / sample. Cells were then washed three times with CyFACS and fixed overnight at 4°C in 100 μl of 2% PFA in PBS. The next day, samples were washed twice with Intracellular Fixation & Permeabilization Buffer (eBioscience), and incubated for 45 minutes at 4°C. After two additional washes with Permeabilization Buffer (eBioscience), samples were blocked for 15 minutes at 4°C in 100 μl of Permeabilization Buffer containing mouse and rat sera. After one additional wash with Permeabilization Buffer, samples were stained with the intracellular CyTOF antibodies

(Table S2) at 4°C for 45 minutes in a volume of 100 μl / sample. Cells were then washed once with CyFACS, and stained for 20 minutes at room temperature with 250 nM of Cell-ID™ Intercalator-IR (Fluidigm). Immediately prior to sample acquisition, cells were washed twice with CyFACS buffer, once with MaxPar® cell staining buffer (Fluidigm), and once with Cell acquisition solution (CAS, Fluidigm). Cells were resuspended in EQ™ Four Element Calibration Beads (Fluidigm) diluted in CAS immediately prior to acquisition on a Helios-upgraded CyTOF2 instrument (Fluidigm) at the UCSF Parnassus flow core facility.

QUANTIFICATION AND STATISTICAL ANALYSIS

CyTOF data analysis

CyTOF datasets, exported as flow cytometry standard (FCS) files, were de-barcoded and normalized according to manufacturer's instructions (Fluidigm). FlowJo software (BD Biosciences) was used to identify CD4+ T cells (live, singlet CD3+CD19-CD4+CD8-) and CD8+ T cells (live, singlet CD3+CD19-CD4-CD8+) among all analyzed samples. IFNγ+ in the stimulated samples were considered to be the SARS-CoV-2-responsive cells. For high-dimensional analyses of SARS-CoV-2-specific T cells among the stimulated samples, we excluded samples with an insufficient number of events (≤ 3) to limit skewing of the data. Manual gating analysis was initially performed using FlowJo, and then select populations were exported as FCS files and then imported into R software as GatingSet objects. Using the *CytoExploreR* package, 2D-gates were manually drawn on the imported samples. The 2D dot plots and statistical results were exported for data visualization, bar-graph generation, and statistical comparisons as previously described (https://github.com/DillonHammill/CytoExploreR). High-dimensional analyses (MDS, tSNE, and flowSOM) were performed using R software by implementing a CyTOF workflow recently described (Nowicka et al., 2017).

For MDS plot generation, we used the plotMDS function from the *limma* package with default settings. Euclidean distances between all samples were calculated using the arcsinh-transformed median expression levels of the lineage and functional markers listed below.

CD8	Lineage (Only for CD8 subset)
CD4	Lineage (Only for CD4 subset)
CD161	Lineage
HLADR	Lineage
CD45RO	Lineage
CD69	Lineage
CRTH2	Lineage
PD1	Lineage
CXCR5	Lineage
CD27	Lineage
CD3	Lineage
CD2	Lineage
CD62L	Lineage
CCR6	Lineage
OX40	Lineage
CD28	Lineage
CD127	Lineage
RORγt	Lineage
CXCR4	Lineage
CTLA4	Lineage
NFAT	Lineage
CCR5	Lineage
CD137	Lineage
CD95	Lineage
ICOS	Lineage
CD49d	Lineage
CD7	Lineage
Tbet	Lineage
TIGIT	Lineage
CCR7	Lineage
CD45RA	Lineage
CD57	Lineage
CD38	Lineage
α4β7	Lineage
CD25	Lineage
IFNγ	Function
IL6	Function
IL4	Function
IL17	Function

The first (MDS1) and second (MDS2) MDS dimensions were plotted to show the dissimilarities between samples from the indicated conditions as described (Ritchie et al., 2015).

tSNE was performed using the Trsne function from the *Rtsne* package using arcsinh-transformed expression of lineage markers (no PCA step, iterations = 1000, perplexity = 30, theta = 0.5). Events corresponding to unstimulated T cells were down-sampled to 1000 cells per sample, and SARS-CoV-2-specific cells (cell numbers ranging from 4 to 229 per sample) were all included in the tSNE analyses without down-sampling. Each cell was displayed in a tSNE plot for dimension reduction visualization and colored with arcsinh-transformed cell marker expression as heatmaps, or pseudo-colored by the appropriate group.

Unsupervised cell subset clustering was performed using FlowSOM (Van Gassen et al., 2015) and *ConsensusClusterPlus* packages using arcsinh-transformed expression levels of the lineage markers indicated above (Wilkerson and Hayes, 2010). For clustering of SARS-CoV-2-specific T cells, we set the meta-cluster number to 8 and cluster number to 40. The frequency of each cluster within each sample was calculated using the following equation:

(Frequency of cluster in specified sample) = (Cell count of cluster / Total cell count of specified sample)

This was then converted to a percentage by multiplying by 100. The percentages of each cluster from the selected samples were plotted as box plots with jittered points, followed by statistical analysis between the groups. To compare the abundance distribution of clusters between groups, frequencies of clusters in samples from each group were normalized using the equation below:

(Normalized frequency of cluster in specified sample) = (Frequency of cluster in specified sample/ Total number of samples in each group)

This was then converted to a percentage by multiplying by 100, and plotted as stacked bar charts.

Statistical Analysis

The statistical tests used in comparison of groups are indicated within the figure legends. For 2-group comparisons, student's t-tests were performed and p-values were adjusted for multiple testing using the Holm-Sidak method where applicable. For comparisons of 3 or more groups, significance between groups was first evaluated by one-way ANOVA, and then the p-values were adjusted for multiple testing using the Holm-Sidak method where applicable. For datasets with significant ANOVA-adjusted p-values (≤ 0.05), we performed Tukey's honestly significant difference (HSD) post-hoc test to determine the p-values between individual groups.

REFERENCES

Abu-Raddad, L.J., Chemaitelly, H., Butt, A.A., and National Study Group for, C.-V. (2021). Effectiveness of the BNT162b2 Covid-19 Vaccine against the B.1.1.7 and B.1.351 Variants. N. Engl. J. Med.

Bacchus-Souffan, C., Fitch, M., Symons, J., Abdel-Mohsen, M., Reeves, D.B., Hoh, R., Stone, M., Hiatt, J., Kim, P., Chopra, A.*, et al.* (2021). Relationship between CD4 T cell turnover, cellular differentiation and HIV persistence during ART. PLoS Pathog. *17*, e1009214.

Cavrois, M., Banerjee, T., Mukherjee, G., Raman, N., Hussien, R., Rodriguez, B.A., Vasquez, J., Spitzer, M.H., Lazarus, N.H., Jones, J.J.*, et al.* (2017). Mass Cytometric Analysis of HIV Entry, Replication, and Remodeling in Tissue CD4+ T Cells. Cell Rep. *20*, 984-998.

Cele, S., Gazy, I., Jackson, L., Hwa, S.H., Tegally, H., Lustig, G., Giandhari, J., Pillay, S., Wilkinson, E., Naidoo, Y.*, et al.* (2021). Escape of SARS-CoV-2 501Y.V2 from neutralization by convalescent plasma. Nature.

Chen, G., Wu, D., Guo, W., Cao, Y., Huang, D., Wang, H., Wang, T., Zhang, X., Chen, H., Yu, H.*, et al.* (2020). Clinical and immunological features of severe and moderate coronavirus disease 2019. J. Clin. Invest. *130*, 2620-2629.

Collier, D.A., De Marco, A., Ferreira, I., Meng, B., Datir, R., Walls, A.C., Kemp, S.S., Bassi, J., Pinto, D., Fregni, C.S.*, et al.* (2021). Sensitivity of SARS-CoV-2 B.1.1.7 to mRNA vaccine-elicited antibodies. Nature.

Dan, J.M., Mateus, J., Kato, Y., Hastie, K.M., Yu, E.D., Faliti, C.E., Grifoni, A., Ramirez, S.I., Haupt, S., Frazier, A.*, et al.* (2021). Immunological memory to SARS-CoV-2 assessed for up to 8 months after infection. Science *371*.

Davies, N.G., Jarvis, C.I., Group, C.C.-W., Edmunds, W.J., Jewell, N.P., Diaz-Ordaz, K., and Keogh, R.H. (2021). Increased mortality in community-tested cases of SARS-CoV-2 lineage B.1.1.7. Nature.

Ebinger, J.E., Fert-Bober, J., Printsev, I., Wu, M., Sun, N., Figueiredo, J.C., Eyk, J.E.V., Braun, J.G., Cheng, S., and Sobhani, K. (2021). Prior COVID-19 Infection and Antibody Response to Single Versus Double Dose mRNA SARS-CoV-2 Vaccination. medRxiv.

Edara, V.V., Norwood, C., Floyd, K., Lai, L., Davis-Gardner, M.E., Hudson, W.H., Mantus, G., Nyhoff, L.E., Adelman, M.W., Fineman, R.*, et al.* (2021). Infection- and vaccine-induced antibody binding and neutralization of the B.1.351 SARS-CoV-2 variant. Cell Host Microbe *29*, 516-521 e513.

Evavold, B.D., and Allen, P.M. (1991). Separation of IL-4 production from Th cell proliferation by an altered T cell receptor ligand. Science *252*, 1308-1310.

Garcia-Beltran, W.F., Lam, E.C., St Denis, K., Nitido, A.D., Garcia, Z.H., Hauser, B.M., Feldman, J., Pavlovic, M.N., Gregory, D.J., Poznansky, M.C.*, et al.* (2021). Multiple SARS-CoV-2 variants escape neutralization by vaccine-induced humoral immunity. Cell.

Goel, R.R., Apostolidis, S.A., Painter, M.M., Mathew, D., Pattekar, A., Kuthuru, O., Gouma, S., Hicks, P., Meng, W., Rosenfeld, A.M.*, et al.* (2021). Distinct antibody and memory B cell responses in SARS-CoV-2 naive and recovered individuals following mRNA vaccination. Sci Immunol *6*.

Gupta, R.K. (2021). Will SARS-CoV-2 variants of concern affect the promise of vaccines? Nat. Rev. Immunol.

Hoffmann, M., Arora, P., Gross, R., Seidel, A., Hornich, B.F., Hahn, A.S., Kruger, N., Graichen, L., Hofmann-Winkler, H., Kempf, A.*, et al.* (2021). SARS-CoV-2 variants B.1.351 and P.1 escape from neutralizing antibodies. Cell.

Kaech, S.M., Tan, J.T., Wherry, E.J., Konieczny, B.T., Surh, C.D., and Ahmed, R. (2003). Selective expression of the interleukin 7 receptor identifies effector CD8 T cells that give rise to long-lived memory cells. Nat. Immunol. *4*, 1191-1198.

Klenerman, P., and Zinkernagel, R.M. (1998). Original antigenic sin impairs cytotoxic T lymphocyte responses to viruses bearing variant epitopes. Nature *394*, 482-485.

Korber, B., Fischer, W.M., Gnanakaran, S., Yoon, H., Theiler, J., Abfalterer, W., Hengartner, N., Giorgi, E.E., Bhattacharya, T., Foley, B.*, et al.* (2020). Tracking Changes in SARS-CoV-2 Spike: Evidence that D614G Increases Infectivity of the COVID-19 Virus. Cell *182*, 812-827 e819.

Kuzmina, A., Khalaila, Y., Voloshin, O., Keren-Naus, A., Boehm-Cohen, L., Raviv, Y., Shemer-Avni, Y., Rosenberg, E., and Taube, R. (2021). SARS-CoV-2 spike variants exhibit differential infectivity and neutralization resistance to convalescent or post-vaccination sera. Cell Host Microbe *29*, 522-528 e522.

Lederer, K., Castano, D., Gomez Atria, D., Oguin, T.H., 3rd, Wang, S., Manzoni, T.B., Muramatsu, H., Hogan, M.J., Amanat, F., Cherubin, P.*, et al.* (2020). SARS-CoV-2 mRNA Vaccines Foster Potent Antigen-Specific Germinal Center Responses Associated with Neutralizing Antibody Generation. Immunity *53*, 1281-1295 e1285.

Ma, T., Luo, X., George, A.F., Mukherjee, G., Sen, N., Spitzer, T.L., Giudice, L.C., Greene, W.C., and Roan, N.R. (2020). HIV efficiently infects T cells from the endometrium and remodels them to promote systemic viral spread. Elife *9*, e55487.

Ma, T., Ryu, H., McGregor, M., Babcock, B., Neidleman, J., Xie, G., George, A.F., Frouard, J., Murray, V., Gill, G.*, et al.* (2021). Protracted yet coordinated differentiation of long-lived SARS-CoV-2-specific CD8+ T cells during COVID-19 convalescence. bioRxiv *2021.04.28.441880*.

Madhi, S.A., Baillie, V., Cutland, C.L., Voysey, M., Koen, A.L., Fairlie, L., Padayachee, S.D., Dheda, K., Barnabas, S.L., Bhorat, Q.E.*, et al.* (2021). Efficacy of the ChAdOx1 nCoV-19 Covid-19 Vaccine against the B.1.351 Variant. N. Engl. J. Med.

Mamazhakypov, A., Viswanathan, G., Lawrie, A., Schermuly, R.T., and Rajagopal, S. (2019). The role of chemokines and chemokine receptors in pulmonary arterial hypertension. Br. J. Pharmacol. *178*, 72-89.

Muik, A., Wallisch, A.K., Sanger, B., Swanson, K.A., Muhl, J., Chen, W., Cai, H., Maurus, D., Sarkar, R., Tureci, O.*, et al.* (2021). Neutralization of SARS-CoV-2 lineage B.1.1.7 pseudovirus by BNT162b2 vaccine-elicited human sera. Science *371*, 1152-1153.

Neidleman, J., Luo, X., Frouard, J., Xie, G., Gill, G., Stein, E.S., McGregor, M., Ma, T., George, A.F., Kosters, A.*, et al.* (2020a). SARS-CoV-2-Specific T Cells Exhibit Phenotypic Features of Helper Function, Lack of Terminal Differentiation, and High Proliferation Potential. Cell Rep Med *1*, 100081.

Neidleman, J., Luo, X., Frouard, J., Xie, G., Hsiao, F., Ma, T., Morcilla, V., Lee, A., Telwatte, S., Thomas, R.*, et al.* (2020b). Phenotypic analysis of the unstimulated in vivo HIV CD4 T cell reservoir. Elife *9*, e55487.

Neidleman, J., Luo, X., George, A.F., McGregor, M., Yang, J., Yun, C., Murray, V., Gill, G., Greene, W.C., Vasquez, J.*, et al.* (2021). Distinctive features of SARS-CoV-2-specific T cells predict recovery from severe COVID-19. medRxiv *2021.01.22.21250054*.

Nowicka, M., Krieg, C., Crowell, H.L., Weber, L.M., Hartmann, F.J., Guglietta, S., Becher, B., Levesque, M.P., and Robinson, M.D. (2017). CyTOF workflow: differential discovery in high-throughput high-dimensional cytometry datasets. F1000Res *6*, 748.

Planas, D., Bruel, T., Grzelak, L., Guivel-Benhassine, F., Staropoli, I., Porrot, F., Planchais, C., Buchrieser, J., Rajah, M.M., Bishop, E.*, et al.* (2021). Sensitivity of infectious SARS-CoV-2 B.1.1.7 and B.1.351 variants to neutralizing antibodies. Nat. Med.

Plante, J.A., Mitchell, B.M., Plante, K.S., Debbink, K., Weaver, S.C., and Menachery, V.D. (2021). The variant gambit: COVID-19's next move. Cell Host Microbe *29*, 508-515.

Redd, A.D., Nardin, A., Kared, H., Bloch, E.M., Pekosz, A., Laeyendecker, O., Abel, B., Fehlings, M., Quinn, T.C., and Tobian, A.A. (2021). CD8+ T cell responses in COVID-19 convalescent individuals target conserved epitopes from multiple prominent SARS-CoV-2 circulating variants. medRxiv.

Ritchie, M.E., Phipson, B., Wu, D., Hu, Y., Law, C.W., Shi, W., and Smyth, G.K. (2015). limma powers differential expression analyses for RNA-sequencing and microarray studies. Nucleic Acids Res. *43*, e47.

Rydyznski Moderbacher, C., Ramirez, S.I., Dan, J.M., Grifoni, A., Hastie, K.M., Weiskopf, D., Belanger, S., Abbott, R.K., Kim, C., Choi, J.*, et al.* (2020). Antigen-Specific Adaptive Immunity to SARS-CoV-2 in Acute COVID-19 and Associations with Age and Disease Severity. Cell *183*, 996-1012 e1019.

Skelly, D.T., Harding, A.C., Gilbert-Jaramillo, J., Knight, M.L., Longet, S., Brown, A., Adele, S., Adland, E., Brown, H., Team, M.L.*, et al.* (2021). Vaccine-induced immunity provides more robust heterotypic immunity than natural infection to emerging SARS-CoV-2 variants of concern. Research Square.

Sloan-Lancaster, J., and Allen, P.M. (1996). Altered peptide ligand-induced partial T cell activation: molecular mechanisms and role in T cell biology. Annu. Rev. Immunol. *14*, 1-27.

Soresina, A., Moratto, D., Chiarini, M., Paolillo, C., Baresi, G., Foca, E., Bezzi, M., Baronio, B., Giacomelli, M., and Badolato, R. (2020). Two X-linked agammaglobulinemia patients develop pneumonia as COVID-19 manifestation but recover. Pediatr. Allergy Immunol.

Stamatatos, L., Czartoski, J., Wan, Y.H., Homad, L.J., Rubin, V., Glantz, H., Neradilek, M., Seydoux, E., Jennewein, M.F., MacCamy, A.J.*, et al.* (2021). mRNA vaccination boosts cross-variant neutralizing antibodies elicited by SARS-CoV-2 infection. Science.

Tarke, A., Sidney, J., Methot, N., Zhang, Y., Dan, J.M., Goodwin, B., Rubiro, P., Sutherland, A., da Silva Antunes, R., Frazier, A.*, et al.* (2021). Negligible impact of SARS-CoV-2 variants on CD4 (+) and CD8 (+) T cell reactivity in COVID-19 exposed donors and vaccinees. bioRxiv.

Van Gassen, S., Callebaut, B., Van Helden, M.J., Lambrecht, B.N., Demeester, P., Dhaene, T., and Saeys, Y. (2015). FlowSOM: Using self-organizing maps for visualization and interpretation of cytometry data. Cytometry A *87*, 636-645.

Wang, P., Nair, M.S., Liu, L., Iketani, S., Luo, Y., Guo, Y., Wang, M., Yu, J., Zhang, B., Kwong, P.D.*, et al.* (2021). Antibody Resistance of SARS-CoV-2 Variants B.1.351 and B.1.1.7. Nature.

Weissman, D., Alameh, M.G., de Silva, T., Collini, P., Hornsby, H., Brown, R., LaBranche, C.C., Edwards, R.J., Sutherland, L., Santra, S.*, et al.* (2021). D614G Spike Mutation Increases SARS CoV-2 Susceptibility to Neutralization. Cell Host Microbe *29*, 23-31 e24.

Wilkerson, M.D., and Hayes, D.N. (2010). ConsensusClusterPlus: a class discovery tool with confidence assessments and item tracking. Bioinformatics *26*, 1572-1573.

Woodruff, M.C., Ramonell, R.P., Nguyen, D.C., Cashman, K.S., Saini, A.S., Haddad, N.S., Ley, A.M., Kyu, S., Howell, J.C., Ozturk, T.*, et al.* (2020). Extrafollicular B cell responses correlate with neutralizing antibodies and morbidity in COVID-19. Nat. Immunol. *21*, 1506-1516.

Xie, G., Luo, X., Ma, T., Frouard, J., Neidleman, J., Hoh, R., Deeks, S.G., Greene, W.C., and Roan, N.R. (2021). Characterization of HIV-induced remodeling reveals differences in infection susceptibility of memory CD4(+) T cell subsets in vivo. Cell Rep. *35*, 109038.

MAIN FIGURE LEGENDS

Figure 1. SARS-CoV-2-specific T cells elicited by vaccination recognize variants, and in a manner that differs among individuals with prior COVID-19. (**A**) Identification of vaccine-elicited spike-specific T cells. PBMCs before vaccination (Pre-Vac) or 2 weeks after each dose of vaccination were stimulated with spike peptides and assessed by CyTOF 6 hours later for the presence of spike-specific (IFNγ-producing) CD4+ (*left*) or CD8+ (*right*) T cells. The "no peptide" conditions served as negative controls. Shown are longitudinal data from an infection-naïve (PID4101, *top*) and convalescent (PID4112, *bottom*) individual. **(B)** Quantification of the spike-specific CD4+ (*left*) and CD8+ (*right*) T cells recognizing the ancestral (squares), B.1.1.7 (triangles), and B.1.351 (circles) spike peptides in infection-naïve (*top*) and convalescent (*bottom*) individuals before and after vaccination. Note the similar frequencies of T cells responding to all three spike proteins in each donor, the clear boosting of spike-specific CD4+ T cell frequencies in infection-naïve but not convalescent individuals, and the overall higher proportion of responding CD4+ than CD8+ T cells. The dotted line corresponds to the magnitude of the maximal pre-vaccination response in infection-naïve individuals and is considered as background. The y-axes are fitted based upon the maximal post-vaccination response values for each patient group and T cell subset. The *p*-values shown (**$p < 0.01$, ****$p < 0.0001$) were calculated by student's t-test. **(C)** As expected, nucleocapsid-specific T cell responses are generally low over the course of vaccination, with the exception of convalescent donor PID4112. Shown are the frequencies of nucleocapsid-specific CD4+ (*left*) and CD8+ (*right*) T cells, as measured by IFNγ production upon stimulation with ancestral nucleocapsid peptides, in infection-naïve (*top*) and convalescent (*bottom*) individuals. The dotted line corresponds to the magnitude of the maximal pre-vaccination response infection-naïve individuals, and is considered as the background signal. Y-axes are labeled to match the

corresponding y-axes for spike-specific T cell responses in *panel B*. **(D)** The CD4+ T cell response is boosted by the second vaccine dose to a greater extent in infection-naïve than convalescents individuals. Shown are the frequencies of spike-specific CD4+ (*left*) and CD8+ (*right*) T cells stimulated by the three spike proteins (squares: ancestral; triangles: B.1.1.7; circles: B.1.351) among the infection-naïve (aqua) and convalescent (coral) donors, after removal of outlier PID4112. ****$p < 0.0001$ comparing the infection-naïve vs. convalescent post-dose 2 specimens, were calculated using student's t-test.

Figure 2. SARS-CoV-2-specific CD4+ T cells responding to B.1.1.7 and B.1.351 spike have the same phenotypes as those responding to ancestral spike. (A) Datasets corresponding to spike-specific CD4+ T cells after vaccination were visualized as a multidimensional scaling (MDS) plot. Each datapoint reflects the cumulative phenotypes averaged across all the SARS-CoV-2-specific CD4+ T cells from a single sample. Data for both infection-naïve and convalescent individuals, and for both the post-dose 1 and post-dose 2 timepoints, are shown. The lack of segregation of the cells responding to the ancestral, B.1.1.7, and B.1.351 spike proteins suggest phenotypic similarities. **(B)** Visualization of the datasets by tSNE dot plots. CD4+ T cells responding to ancestral or variant spike stimulation by producing high amounts of IFNγ (*right*) segregate together and away from the total CD4+ T cell population (*left*). Each dot represents one cell. **(C)** CD4+ T cells responding to ancestral spike and its variants are phenotypically similar, as shown by their complete mingling on a tSNE dot plot. **(D, E)** Spike-responding CD4+ T cells are mostly memory cells, as indicated by high CD45RO and low CD45RA expression levels, and include those expressing high levels of Tcm, Tfh, activation, and respiratory tract migration markers. Shown is the tSNE depicted in *panel C* displaying the relative expression levels of the indicated antigens (Red: high; Blue: low). **(F)** CD4+ T cells responding to ancestral spike and its variants distribute in a similar fashion among the 8 clusters identified by flowSOM. Shown on the left is the distribution of T cells responding to ancestral or

variant spike peptides on the tSNE depicted in *panel C,* colored according to the flowSOM clustering. Shown on the right is the quantification of the flowSOM distribution data. No significant differences were observed between the three groups in the distribution of their cells among the 8 clusters, as calculated using a one-way ANOVA and adjusted for multiple testing (n = 8) using Holm-Sidak method ($p > 0.05$).

Figure 3. Differentiation of spike-specific memory CD4+ T cells after vaccination of convalescent individuals. (A) MDS plot depicting datasets corresponding to spike-specific CD4+ T cells in convalescent individuals before and after vaccination. The blue line emphasizes the nearly universal segregation of pre- from post-vaccination samples. **(B)** tSNE contour heatmaps of spike-specific CD4+ T cells from convalescent individuals demonstrate phenotypic differences between the pre- and post-vaccination cells. Cell densities are represented by color. **(C)** tSNE dot plot of spike-specific CD4+ T cells from convalescent individuals, demonstrating the distinct localization of the pre-vaccination cells in the upper right. **(D)** Spike-specific CD4+ T cells are phenotypically distinct between the pre- and post-vaccination specimens. Shown are tSNE plots depicting cells from the three indicated timepoints, colored according to the cells' cluster classification as determined by flowSOM. **(E)** The distribution of spike-specific CD4+ T cells classified as flowSOM clusters differs between the pre- and post-vaccination timepoints. **(F)** Three clusters of spike-specific CD4+ T cells are differentially abundant between the pre- and post-vaccination specimens. $^{**}p < 0.01$, $^{***}p < 0.001$, $^{****}p < 0.0001$ as determined by one-way ANOVA and adjusted for multiple testing (n = 8) using the Holm-Sidak method followed by Tukey's honestly significant difference (HSD) post-hoc test. **(G)** Vaccination of convalescent individuals increases the proportion of spike-specific CD4+ T cells that are activated (CD38+ and HLADR+), and that express co-stimulatory receptors (ICOS+ and Ox40+) and checkpoint molecules (PD1+ and CTL4+). The percentages of cells co-expressing the activation markers CD38 and HLADR, the co-stimulatory molecules ICOS and Ox40, or the checkpoint molecules

PD1 and CTLA4, were assessed among spike-specific CD4+ T cells from convalescent donors. *p < 0.05, **p < 0.01, ****p < 0.0001 as determined by one-way ANOVA followed by Tukey's HSD post-hoc test.

Figure 4. Phenotypic features of spike-specific CD4+ T cells differ between infection-naïve and convalescent individuals after vaccination. (A) The frequency of spike-specific CD4+ T cells is similar in infection-naïve and convalescent individuals two weeks after the second vaccination dose. Note that when convalescent donor PID4112, who had an unusually high pre-vaccination frequency of spike-specific CD4+ T cells (Fig. 1D), was excluded, the frequency was significantly lower among the convalescents. **(B)** MDS plots of the phenotypes of spike-specific CD4+ T cells in infection-naïve and convalescent individuals after first and second dose vaccinations. The blue divider emphasizes the general segregation of infection-naïve from convalescent donors, which is more apparent after the second dose. **(C)** tSNE contour heatmaps of spike-specific CD4+ T cells from infection-naïve and convalescent individuals, after first and second dose vaccinations, highlighting the phenotypic differences between the two groups of patients, particularly after the second dose. Cell densities are represented by color. **(D)** tSNE dot plot of spike-specific CD4+ T cells from infection-naïve and convalescent individuals after second dose of vaccination, demonstrating the segregation of the cells from the two groups of patients. **(E)** Spike-specific CD4+ T cells are phenotypically distinct between the infection-naïve and convalescent individuals. Shown are tSNE plots depicting cells after the second dose of vaccination, colored according to the cells' cluster classification as determined by flowSOM. **(F)** The distribution of spike-specific CD4+ T cells into flowSOM clusters differs between the infection-naïve and convalescent individuals after the second vaccine dose. **(G)** Two clusters of spike-specific CD4+ T cells (A1 and A3) are differentially represented between infection-naïve and convalescent individuals after the second dose of vaccination. *p < 0.05, as

determined by student's t-tests adjusted for multiple testing (n = 8) using the Holm-Sidak method.

Figure 5. The post-vaccination spike-specific CD4+ T cells of convalescents harbor phenotypic features of elevated longevity and tissue homing. (A) Spike-specific CD4+ T cells from convalescent vaccinated individuals harbor higher proportions of Tcm and lower proportions of Ttm than those from infection-naïve vaccinated individuals. The proportions of Tn (CD45RO-CD45RA+CCR7+CD95-), Tscm (CD45RO-CD45RA+CCR7+CD95+), Temra (CD45RO-CD45RA+CCR7-), Tcm (CD45RO+CD45RA-CCR7+CD27+), Tem (CD45RO+CD45RA-CCR7-CD27-), and Ttm (CD45RO+CD45RA-CCR7-CD27+) cells among spike-specific CD4+ T cells were determined by manual gating. **$p < 0.01$, ****$p < 0.0001$, ns = non-significant, as determined by student's t-test. **(B)** The proportions of Tfh (CD45RO+CD45RA-PD1+CXCR5+) and Treg (CD45RO+CD45RA-CD25+CD127^{low}) among spike-specific CD4+ T cells are similar in infection-naïve vs. convalescent individuals after vaccination. ns = non-significant, as determined by student's t-test. **(C)** Spike-specific CD4+ T cells expressing the homeostatic proliferation marker CD127 and lacking expression of the terminal differentiation marker CD57 are more frequent in vaccinated convalescent than vaccinated infection-naïve individuals. ***$p < 0.001$, as determined by student's t-test. **(D)** Spike-specific CD4+ T cells expressing the lymph node homing receptors CCR7 and CD62L are more frequent in vaccinated convalescent individuals. *$p < 0.05$, as determined by student's t-test. **(E)** Spike-specific CD4+ T cells expressing CXCR4, which directs cells to tissues including the lung, and CD69, a marker of T cell activation and tissue residence, are more frequent in convalescent vaccinated individuals. **$p < 0.01$, as determined by student's t-test. For *panels C-E*, the dot plots on the left show concatenated data from all the donors. **(F)** The proportions of CCR7+CD62L+ and CXCR4+CD69+ cells among spike-specific CD4+ T cells associate negatively with the frequencies of spike-specific CD4+ T cells after the second dose of

vaccination (correlation coefficient (R) < 0). *P*-values were calculated using t distribution with n-2 degrees of freedom. **(G)** Expression levels (reported as mean signal intensity, or MSI) of CCR7 and CD62L among spike-specific CD4+ T cells associate negatively (R < 0) with overall frequencies of spike-specific CD4+ T cells after the second dose of vaccination. *P*-values were calculated using t distribution with n-2 degrees of freedom. The 95% confidence intervals of the regression lines in the scatter plots of *panels F-G* are shaded in grey. **(H)** CCR7+CD62L+ and CXCR4+CD69+ CD4+ T cells are more frequent in nasopharynx than blood. Unstimulated CD4+ T cells from the blood (*grey*) or from an intranasal swab (*red*) were obtained on the same day from PID4101 and then phenotyped by CyTOF. Numbers indicate the percentages of the corresponding cell population within the gate. Results are gated on live, singlet CD3+CD4+CD8- cells.

Figure 6. Unique phenotypic features of post-vaccination spike-specific CD4+ T cells are not due to different number of antigen exposures. (A) The proportions of CD57-CD127+, CCR7+CD62L+, and CXCR4+CD69+ cells among spike-specific CD4+ T cells are similar after the first and second doses of vaccination in convalescent individuals. **(B)** The proportions of CD57-CD127+, CCR7+CD62L+, CXCR4+CD69+, Tcm, and Ttm among spike-specific CD4+ T cells differ in infection-naïve individuals after their second vaccination dose compared to convalescent individuals after their first vaccination dose. Note that the groups compared here both were exposed to spike antigen twice and analyzed at similar timepoints after the second exposure. *p < 0.05, **p < 0.01, ***p < 0.001, ns = non-significant, as determined student's t-test.

SUPPLEMENTARY FIGURE LEGENDS

Figure S1. Six-hour stimulation with spike peptides does not induce significant expression of activation markers in SARS-CoV-2-specific T cells. (A) CD4+ T cells were assessed for co-expression of the activation-induced markers (AIM) Ox40 and 4-1BB following 6 hours of stimulation with ancestral spike peptides using PBMC specimens from a representative infection-naïve individual (PID4197) before vaccination (Pre-Vac), or two weeks after dose 1 or dose 2 of vaccination. **(B)** CD8+ T cells were assessed for co-expression of the AIM CD69 and 4-1BB following 6 hours of stimulation, using same specimens as *panel A*. Baseline specimens not treated with peptide are shown as a comparison control. Numbers correspond to percentages of cells within the gates. Note that the activated (AIM+) cells that appear in stimulated specimens probably do not reflect peptide-specific stimulation as AIM+ cells are also detected in the baseline specimens.

Figure S2. Expression levels of all CyTOF phenotyping markers are equivalent between CD4+ T cells responding to stimulation by spike from ancestral, B.1.1.7, and B.1.351 spike. Shown are the mean expression levels of each antigen in post-vaccination spike-responding CD4+ T cells quantitated by CyTOF. Each datapoint corresponds to a single specimen. No significant differences were observed in expression levels for any of the antigens between any of the three groups, as assessed by one-way and ANOVA adjusted for multiple testing (n = 39) using the Holm-Sidak method ($p > 0.05$).

Figure S3. Phenotypes of spike-specific CD4+ T cells from infection-naïve individuals are similar following first and second dose of vaccination. (A) MDS plot depicting samples of spike-specific CD4+ T cells in vaccinated infection-naïve individuals, showing interspersion of the cells from the two post-vaccination timepoints. Each dot represents a single specimen. **(B)**

tSNE dot plot of spike-specific CD4+ T cells from vaccinated infection-naïve individuals. Each dot represents a single cell. Although fewer cells are present at the first timepoint, these cells spread over the same regions of the tSNE plot as do the cells from the second timepoint, suggesting phenotypic overlap between the two timepoints. **(C)** Spike-specific CD4+ T cells from vaccinated infection-naïve individuals are phenotypically similar at the first and second vaccination timepoints. Shown are tSNE plots depicting cells from the two timepoints, colored according to the cells' cluster classification as determined by flowSOM. **(D)** Distribution among flowSOM clusters of post-vaccination spike-specific CD4+ T cells from infection-naïve individuals are similar between the two post-vaccination timepoints. **(E)** Lack of enrichment of any clusters of spike-specific T cells in either post-vaccination timepoint relative to the other in vaccinated infection-naïve individuals, as determined using student's t-tests adjusted for multiple testing (n = 8) using Holm-Sidak method. **(F)** The proportions of Tn (CD45RO-CD45RA+CCR7+CD95-), Tscm (CD45RO-CD45RA+CCR7+CD95+), Temra (CD45RO-CD45RA+CCR7-), Tcm (CD45RO+CD45RA-CCR7+CD27+), Tem (CD45RO+CD45RA-CCR7-CD27-), and Ttm (CD45RO+CD45RA-CCR7-CD27+) among spike-specific CD4+ cells differ little in infection-naive individuals after the first vs. second vaccination doses. *$p < 0.05$, ns = non-significant as determined by student's t-test. **(I)** The proportions of Tfh (CD45RO+CD45RA-PD1+CXCR5+) and Treg (CD45RO+CD45RA-CD25+CD127^{low}) among spike-specific CD4+ T cells are similar in infection-naive individuals after the first vs. second vaccination doses. ns = non-significant as determined by student's t-test.

Figure S4. The distribution of spike-specific T cells among the canonical subsets of CD4+ T cells is similar in convalescent individuals pre- and post-vaccination. (A) The proportions of Tn, Tscm, Temra Tcm, Tem, and Ttm among spike-specific CD4+ cells are similar in convalescent individuals before and after vaccination. **(B)** The proportions of Tfh and

Treg among spike-specific CD4+ T cells are similar in convalescent individuals before and after vaccination. Distributions were assessed by one-way ANOVA ($p > 0.05$).

Figure S5. Cluster C3, enriched in pre-vaccination spike-specific CD4+ T cells from convalescent individuals, exhibits low activation phenotypes. Shown are histogram depictions of the expression levels of the indicated activation markers in cluster C1 **(A)** or C3 **(B)**. Both clusters were enriched in cells from the pre-vaccination specimens. While cluster C1 expressed activation markers at levels generally similar to those of total spike-specific CD4+ T cells, cluster C3 expressed low levels of all activation markers. These results suggest that a subset of unactivated, spike-specific CD4+ T cells of the C3 phenotype are depleted after vaccination in convalescent individuals. Shown are concatenated data from all clustered cells from both the pre- and post-vaccination specimens from convalescent participants.

Figure S6. Cluster A3, enriched among spike-specific CD4+ T cells from convalescent vaccinated individuals, express high levels of markers of homeostatic proliferation and tissue homing. (A) Shown are histograms of the expression levels of the alpha chain of the IL7 receptor (CD127), the lymph node homing receptor CCR7, and the chemokine receptor CXCR4 among clusters A1 or A3, both of which were enriched in convalescent relative to infection-naïve individuals after vaccination. Cluster A3 expressed high levels of all three receptors relative to total spike-specific CD4+ T cells. Data were concatenated from all clustered cells. **(B)** Relative expression levels, as depicted by normalized mean signal intensity (MSI), of CD127, CCR7, and CXCR4 among all specimens of spike-specific CD4+ T cells from infection-naïve and convalescent individuals, after the second vaccination dose. $*p < 0.05$, $**p < 0.01$, ns = non-significant, as determined using student's t-tests and corrected for multiple testing ($n = 39$) using the Holm-Sidak method.

Figure S7. Phenotypic features of spike-specific CD8+ T cells from vaccinated, convalescent individuals are unique and differ from those of their CD4+ T cell counterparts. (A-C) MDS (*A*) or tSNE (*B, C*) plots demonstrating phenotypic similarities between spike-specific CD8+ T cells responding to spike from the ancestral, B.1.1.7, or B.1.351 strains. Data are displayed in a format similar to that for CD4+ T cells presented in Fig. 2A-C. **(D)** MDS plot depicting specimens of spike-specific CD8+ T cells in infection-naïve and convalescent individuals after second vaccination dose. The blue divider emphasizes the general segregation of infection-naïve from convalescent donor cells. **(E)** tSNE contour heatmaps depicting spike-specific CD8+ T cells from infection-naïve and convalescent individuals, after the second vaccination dose. Cell densities are represented by color. **(F)** tSNE dot plot of spike-specific CD8+ T cells from infection-naïve and convalescent individuals after second vaccination dose. **(G)** The distribution of spike-specific cells among the main canonical CD8+ T cell subsets (Tn, Tscm, Temra, Tcm, Tem, Ttm) is similar in infection-naïve vs. convalescent individuals after second vaccination dose. **(H)** T cell subsets that were differentially enriched in infection-naïve vs. convalescent individuals among spike-specific CD4+ T cells after second vaccination dose (Fig. 6B) are not differentially enriched among spike-specific CD8+ T cells. Shown are the proportions of cells that are CD127+CD57-, CCR7+CD62L+, or CXCR4+CD69+ cells among spike-specific CD8+ T cells as determined by manual gating. **(I)** Cells co-expressing CD27 and CD38, and CTLA4 and CD137, are elevated among spike-specific CD8+ T cells from vaccinated convalescent individuals relative to vaccinated infection-naïve individuals. *$p < 0.05$, **$p < 0.01$ as determined by student's t-test.

SUPPLEMENTARY TABLES

Table S1. Participant Characteristics

Patient ID	Gender	Age	Prior Infection Status	Vaccine	Days post PCR+ test at pre-vaccination timepoint	Days post vaccine dose #1	Days post vaccine dose #2
PID4101	Female	45	Uninfected	Pfizer/BioNT	NA	13	12
PID4197	Female	76	Uninfected	Pfizer/BioNT	NA	14	13
PID4198	Male	79	Uninfected	Moderna	NA	18	10
PID4199	Female	32	Uninfected	Pfizer/BioNT	NA	14	10
PID4104	Female	33	Convalescent	Moderna	212	14	14
PID4112	Female	59	Convalescent	Moderna	254	16	13
PID4117	Female	51	Convalescent	Pfizer/BioNT	82	16	6
PID4118	Female	39	Convalescent	Pfizer/BioNT	173	18	28

Table S2. List of CyTOF antibodies used in study. Antibodies were either purchased from the indicated vendor or prepared in-house using commercially available MaxPAR conjugation kits per manufacturer's instructions (Fluidigm).

Antigen Target	Clone	Elemental Isotope	Vendor
HLADR	TÜ36	Qdot (112Cd)	Thermofisher
RORγt*	AFKJS-9	115 In	In-house
CD49d (α4)	9F10	141Pr	Fluidigm
CTLA4*	14D3	142Nd	In-house
NFAT*	D43B1	143Nd	Fluidigm
CCR5	NP6G4	144Nd	Fluidigm
CD137	4B4-1	145Nd	In-house
CD95	BX2	146Nd	In-house
CD7	CD76B7	147Sm	Fluidigm
ICOS	C398.4A	148Nd	Fluidigm
Tbet*	4B10	149Sm	In-house
IL4*	MP4-25D2	150Nd	In-house
CD2	TS1/8	151Eu	Fluidigm
IL17*	BL168	152Sm	In-house
CD62L	DREG56	153Eu	Fluidigm
TIGIT	MBSA43	154Sm	Fluidigm
CCR6	11A9	155Gd	In-house
IL6*	MQ2-13A5	156 Gd	In-house
CD8	RPA-T8	157Gd	In-house
CD19	HIB19	157Gd	In-house
CD14	M5E2	157Gd	In-house
OX40	ACT35	158Gd	Fluidigm
CCR7	G043H7	159Tb	Fluidigm
CD28	CD28.2	160Gd	Fluidigm
CD45RO	UCHL1	161Dy	In-house
CD69	FN50	162Dy	Fluidigm
CRTH2	BM16	163Dy	Fluidigm
PD-1	EH12.1	164Dy	In-house
CD127	A019D5	165Ho	Fluidigm
CXCR5	RF8B2	166Er	In-house
CD27	L128	167Er	Fluidigm
IFNγ*	B27	168Er	Fluidigm
CD45RA	HI100	169Tm	Fluidigm
CD3	UCHT1	170Er	Fluidigm
CD57	HNK-1	171Yb	In-house
CD38	HIT2	172Yb	Fluidigm
α4β7	Act1	173Yb	In-house
CD4	SK3	174Yb	Fluidigm
CXCR4	12G5	175Lu	Fluidigm
CD25	M-A251	176Yb	In-house
CD161	NKR-P1A	209 Bi	In-house

*Intracellular antibodies

Figure 1

A.

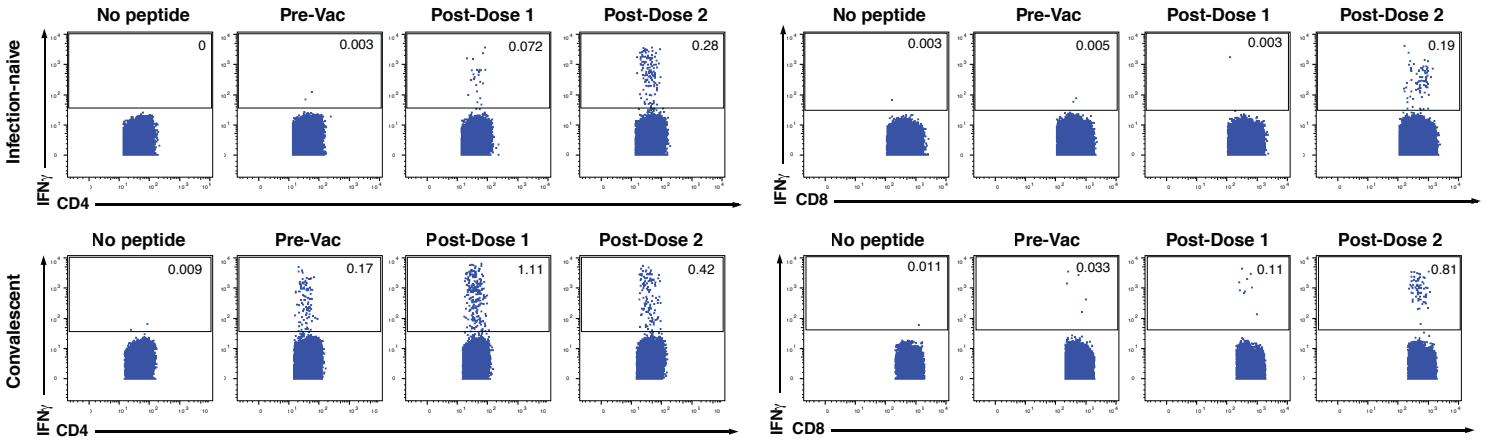

B.

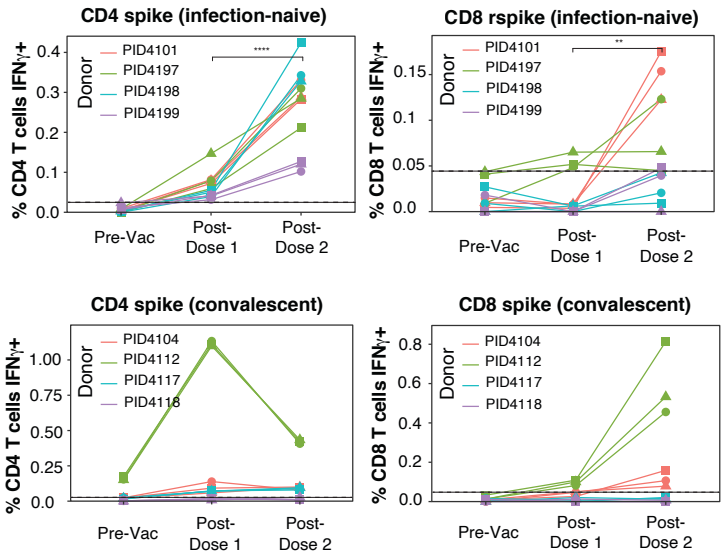

C.

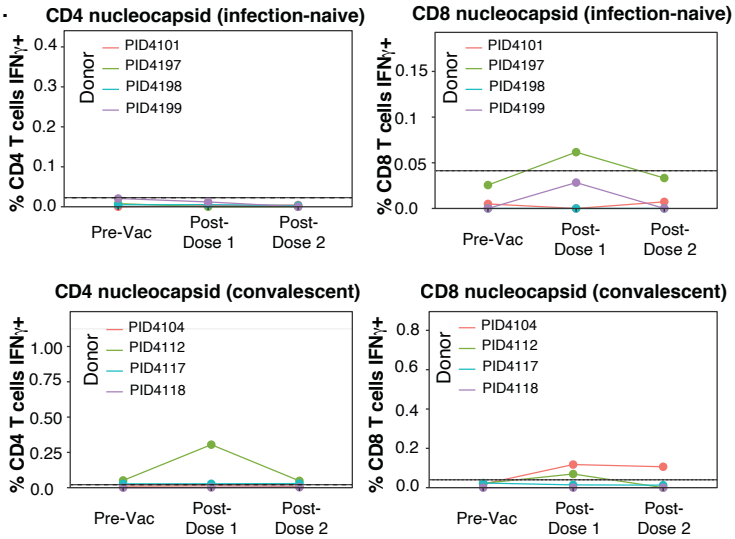

D.

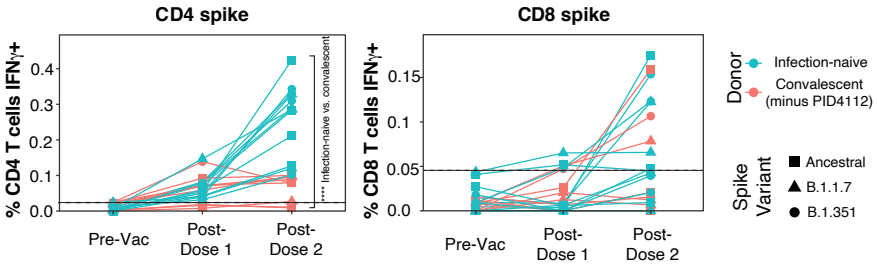

Figure 2

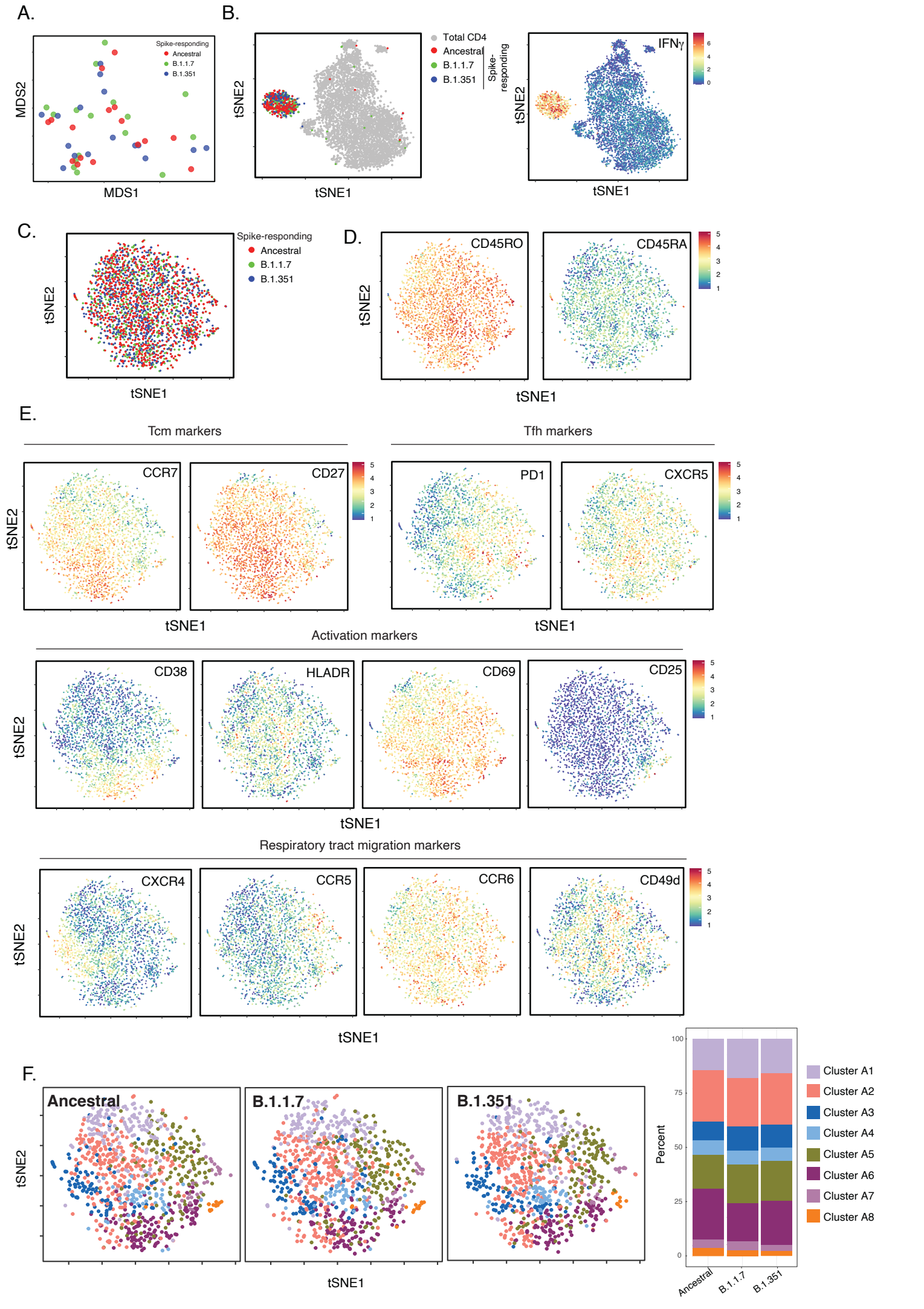
A.
Spike-responding
Ancestral
B.1.1.7
B.1.351
MDS2
MDS1
B.
Total CD4
Ancestral
B.1.1.7
B.1.351
Spike-responding
IFNγ
tSNE2
tSNE1
C.
Spike-responding
Ancestral
B.1.1.7
B.1.351
tSNE2
tSNE1
D.
CD45RO
CD45RA
tSNE2
tSNE1
E.
Tcm markers
CCR7
CD27
Tfh markers
PD1
CXCR5
tSNE2
tSNE1
Activation markers
CD38
HLADR
CD69
CD25
tSNE2
tSNE1
Respiratory tract migration markers
CXCR4
CCR5
CCR6
CD49d
tSNE2
tSNE1
F.
Ancestral
B.1.1.7
B.1.351
tSNE2
tSNE1
Percent
Cluster A1
Cluster A2
Cluster A3
Cluster A4
Cluster A5
Cluster A6
Cluster A7
Cluster A8
Ancestral
B.1.1.7
B.1.351

Figure 3

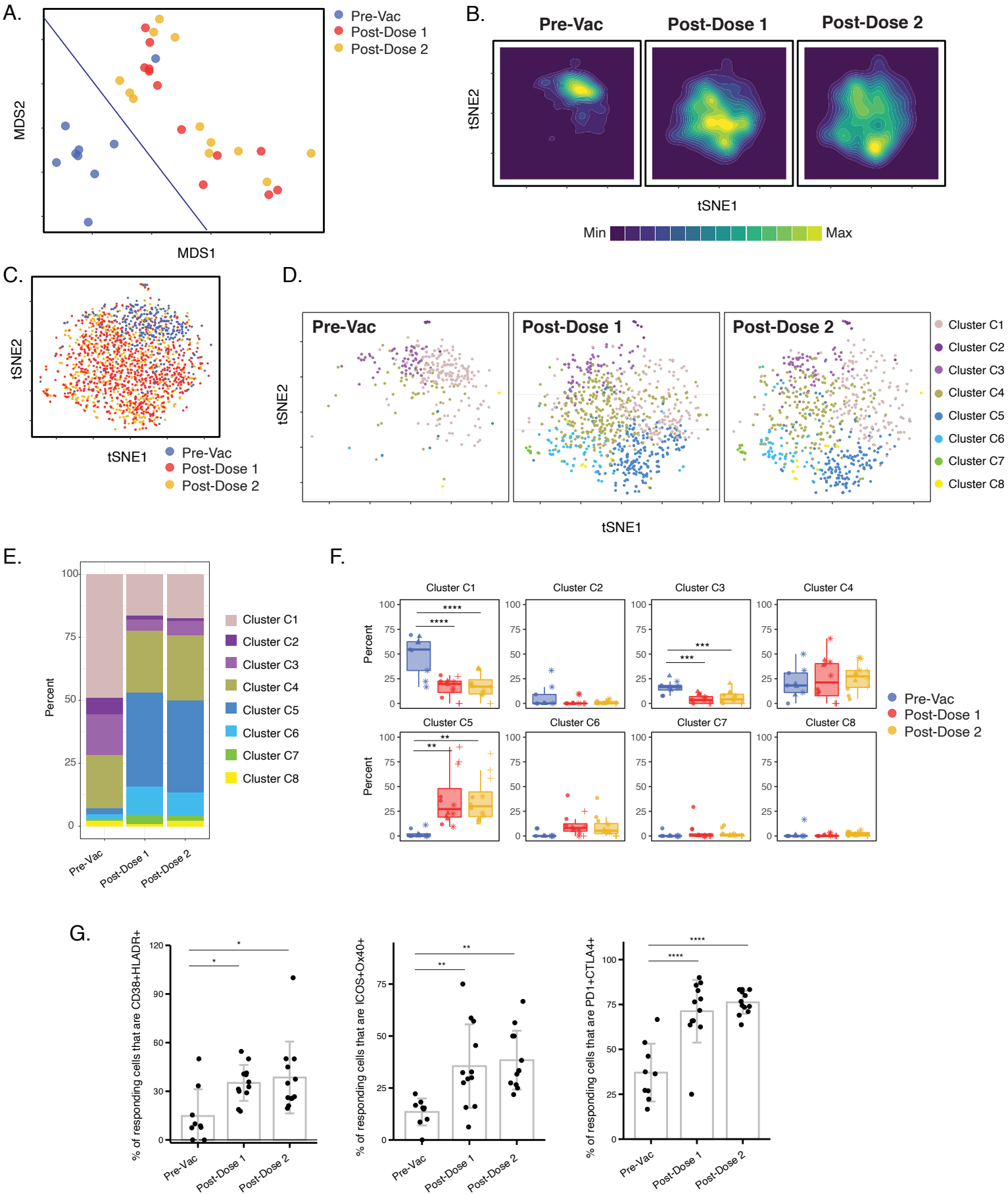
A.
MDS2
MDS1
Pre-Vac
Post-Dose 1
Post-Dose 2
B.
Pre-Vac
Post-Dose 1
Post-Dose 2
tSNE2
tSNE1
Min
Max
C.
tSNE2
tSNE1
Pre-Vac
Post-Dose 1
Post-Dose 2
D.
Pre-Vac
Post-Dose 1
Post-Dose 2
tSNE2
tSNE1
Cluster C1
Cluster C2
Cluster C3
Cluster C4
Cluster C5
Cluster C6
Cluster C7
Cluster C8
E.
Percent
Pre-Vac
Post-Dose 1
Post-Dose 2
F.
Cluster C1
Cluster C2
Cluster C3
Cluster C4
Cluster C5
Cluster C6
Cluster C7
Cluster C8
Percent
Pre-Vac
Post-Dose 1
Post-Dose 2
G.
% of responding cells that are CD38+HLADR+
% of responding cells that are ICOS+Ox40+
% of responding cells that are PD1+CTLA4+
Pre-Vac
Post-Dose 1
Post-Dose 2

Figure 4

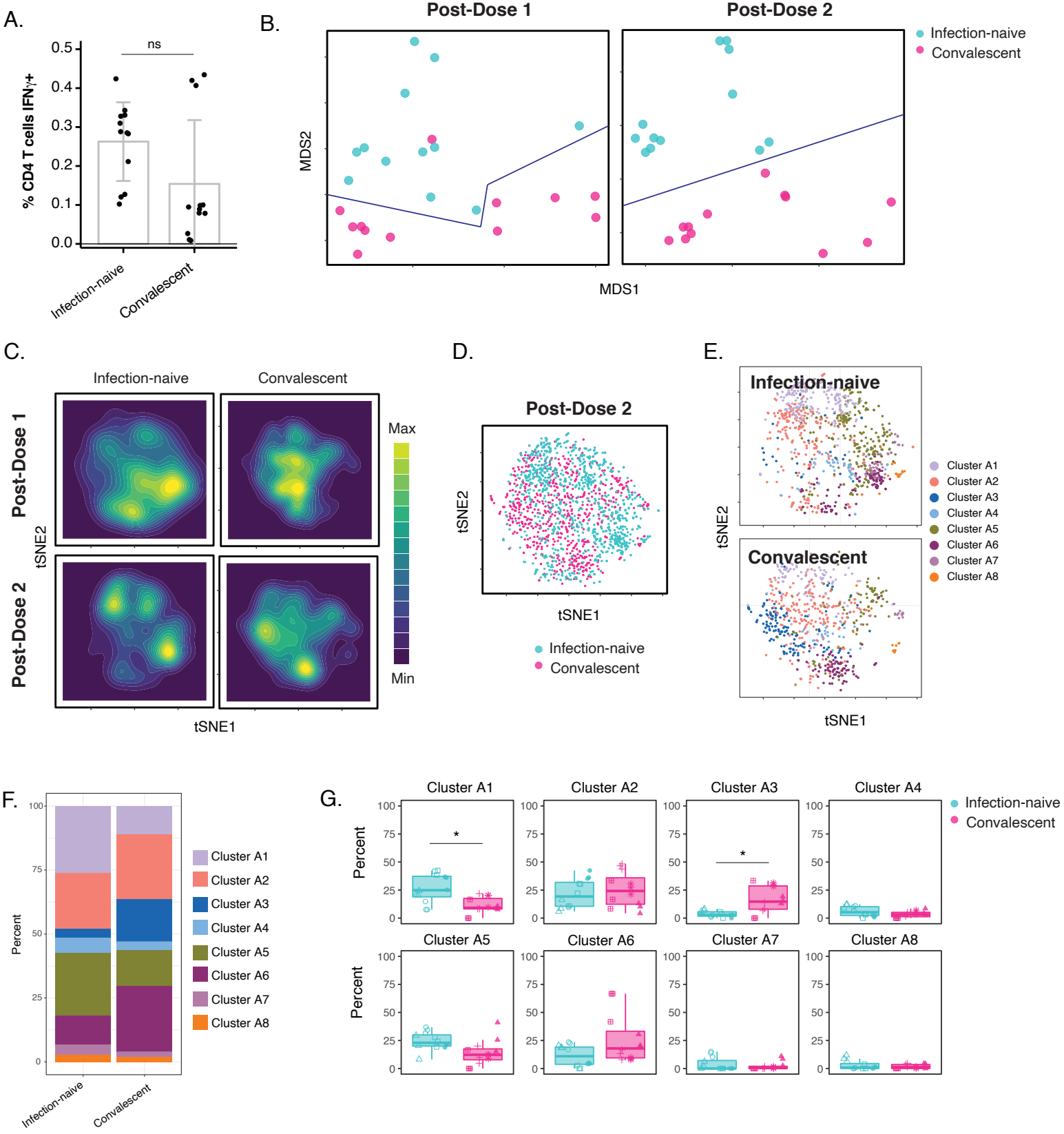
A.
ns
% CD4 T cells IFNγ+
0.5
0.4
0.3
0.2
0.1
0.0
Infection-naive
Convalescent
B.
Post-Dose 1
Post-Dose 2
Infection-naive
Convalescent
MDS2
MDS1
C.
Infection-naive
Convalescent
Post-Dose 1
Post-Dose 2
tSNE2
tSNE1
Max
Min
D.
Post-Dose 2
tSNE2
tSNE1
Infection-naive
Convalescent
E.
Infection-naive
Convalescent
tSNE2
tSNE1
Cluster A1
Cluster A2
Cluster A3
Cluster A4
Cluster A5
Cluster A6
Cluster A7
Cluster A8
F.
Percent
100
75
50
25
0
Infection-naive
Convalescent
Cluster A1
Cluster A2
Cluster A3
Cluster A4
Cluster A5
Cluster A6
Cluster A7
Cluster A8
G.
Cluster A1
Cluster A2
Cluster A3
Cluster A4
Cluster A5
Cluster A6
Cluster A7
Cluster A8
Percent
*
*
Infection-naive
Convalescent

Figure 5

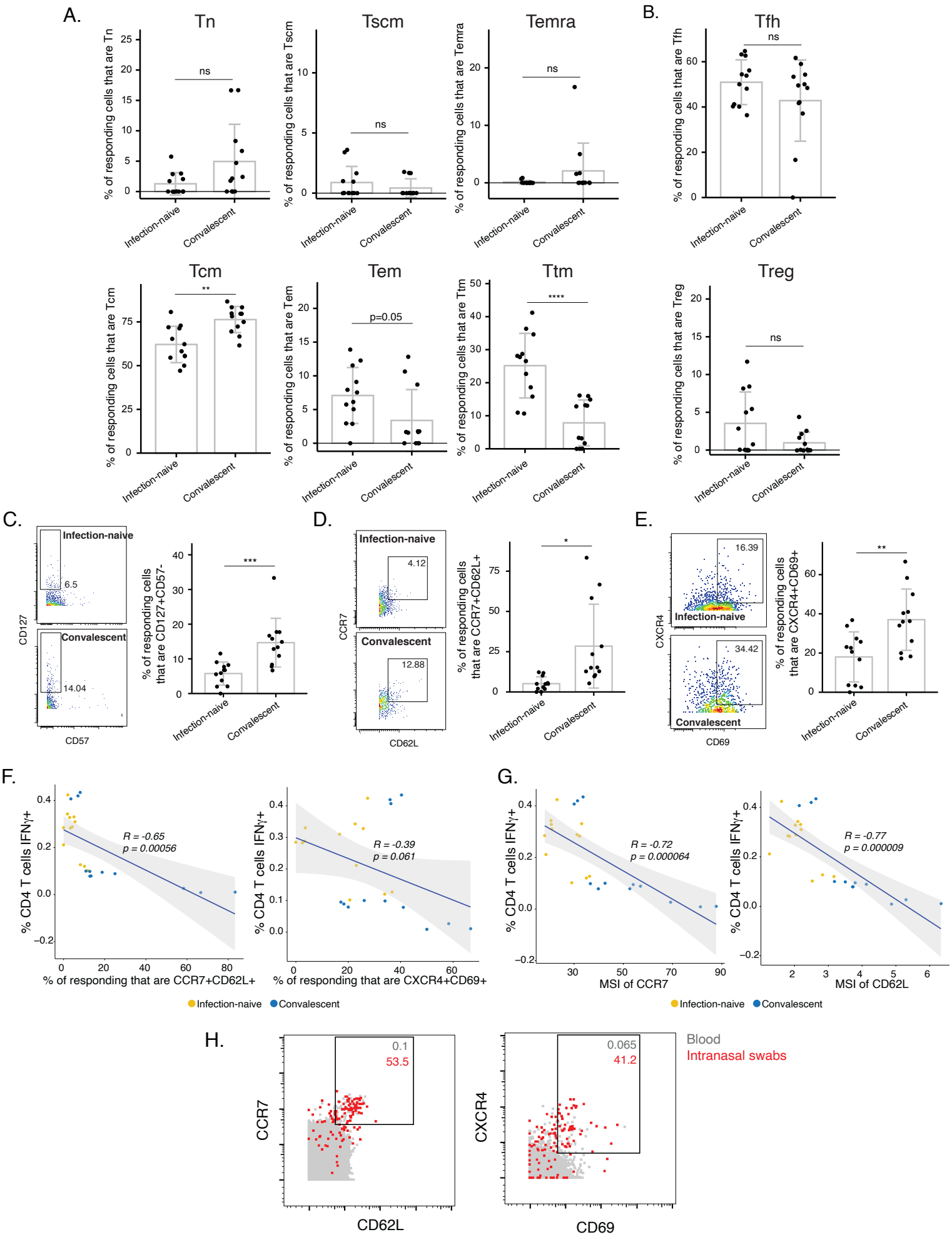
A.
Tn
Tscm
Temra
B.
Tfh
Tcm
Tem
Ttm
Treg
% of responding cells that are Tn
% of responding cells that are Tscm
% of responding cells that are Temra
% of responding cells that are Tfh
% of responding cells that are Tcm
% of responding cells that are Tem
% of responding cells that are Ttm
% of responding cells that are Treg
ns
**
p=0.05
****
Infection-naive
Convalescent
C.
Infection-naive
6.5
Convalescent
14.04
CD127
CD57
% of responding cells that are CD127+CD57-
***
D.
Infection-naive
4.12
Convalescent
12.88
CCR7
CD62L
% of responding cells that are CCR7+CD62L+
*
E.
16.39
Infection-naive
34.42
Convalescent
CXCR4
CD69
% of responding cells that are CXCR4+CD69+
**
F.
% CD4 T cells IFNγ+
R = -0.65
p = 0.00056
% of responding that are CCR7+CD62L+
R = -0.39
p = 0.061
% of responding that are CXCR4+CD69+
Infection-naive
Convalescent
G.
R = -0.72
p = 0.000064
MSI of CCR7
R = -0.77
p = 0.000009
MSI of CD62L
Infection-naive
Convalescent
H.
0.1
53.5
CCR7
CD62L
0.065
41.2
CXCR4
CD69
Blood
Intranasal swabs

Figure 6

A.

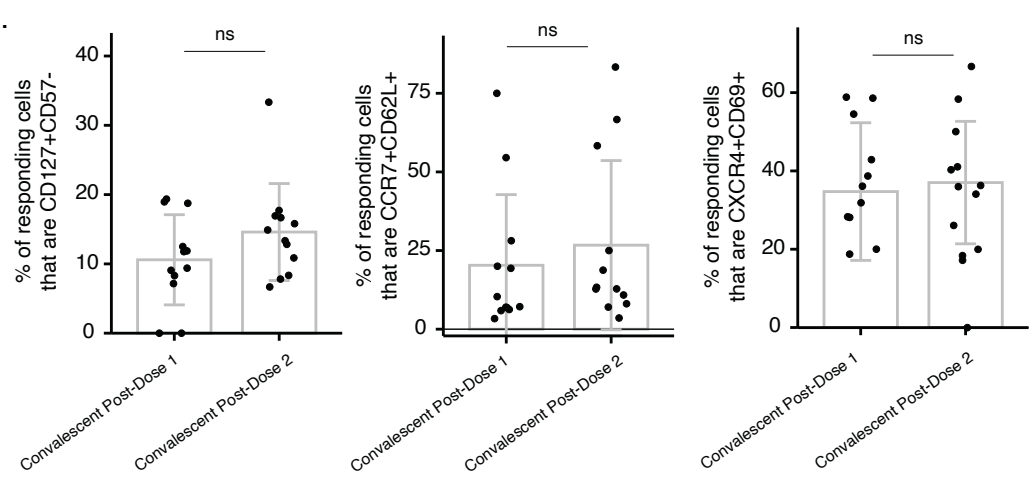
ns
% of responding cells that are CD127+CD57-
0
10
20
30
40
Convalescent Post-Dose 1
Convalescent Post-Dose 2
ns
% of responding cells that are CCR7+CD62L+
0
25
50
75
Convalescent Post-Dose 1
Convalescent Post-Dose 2
ns
% of responding cells that are CXCR4+CD69+
0
20
40
60
Convalescent Post-Dose 1
Convalescent Post-Dose 2

B.

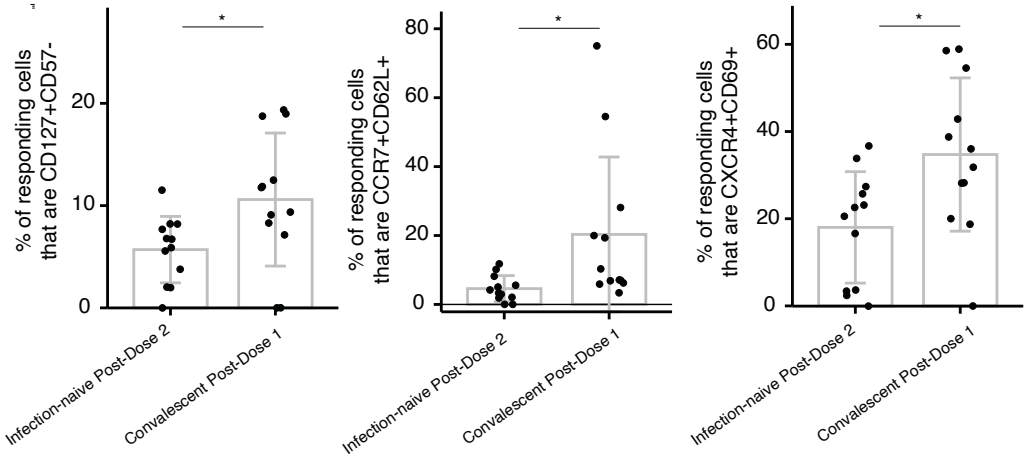
*
% of responding cells that are CD127+CD57-
0
10
20
Infection-naive Post-Dose 2
Convalescent Post-Dose 1
*
% of responding cells that are CCR7+CD62L+
0
20
40
60
80
Infection-naive Post-Dose 2
Convalescent Post-Dose 1
*
% of responding cells that are CXCR4+CD69+
0
20
40
60
Infection-naive Post-Dose 2
Convalescent Post-Dose 1

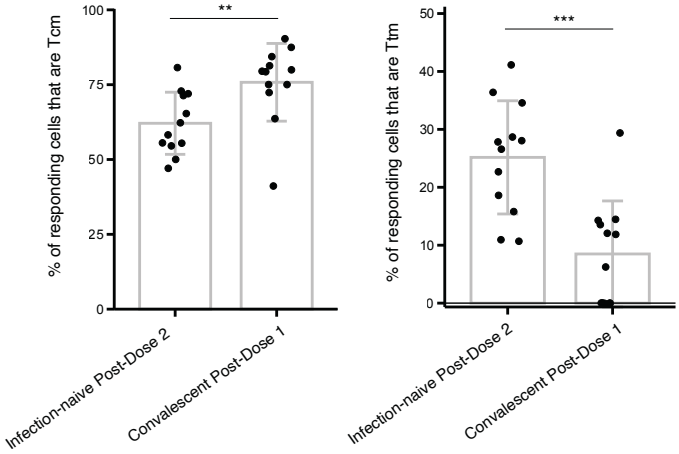
**
% of responding cells that are Tcm
0
25
50
75
100
Infection-naive Post-Dose 2
Convalescent Post-Dose 1
***
% of responding cells that are Ttm
0
10
20
30
40
50
Infection-naive Post-Dose 2
Convalescent Post-Dose 1

Figure S1

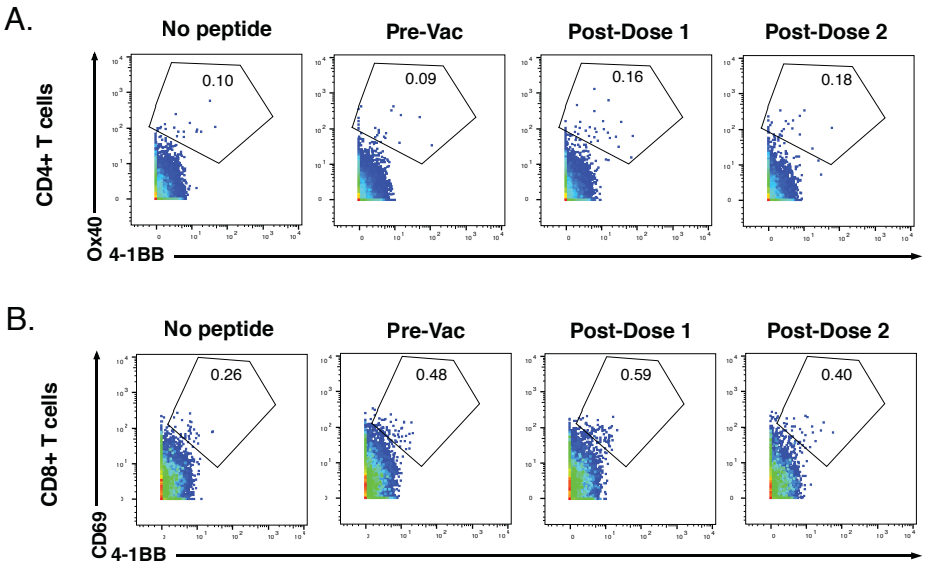
A.
No peptide
Pre-Vac
Post-Dose 1
Post-Dose 2
CD4+ T cells
0.10
0.09
0.16
0.18
Ox40
4-1BB
B.
No peptide
Pre-Vac
Post-Dose 1
Post-Dose 2
CD8+ T cells
0.26
0.48
0.59
0.40
CD69
4-1BB

Figure S2

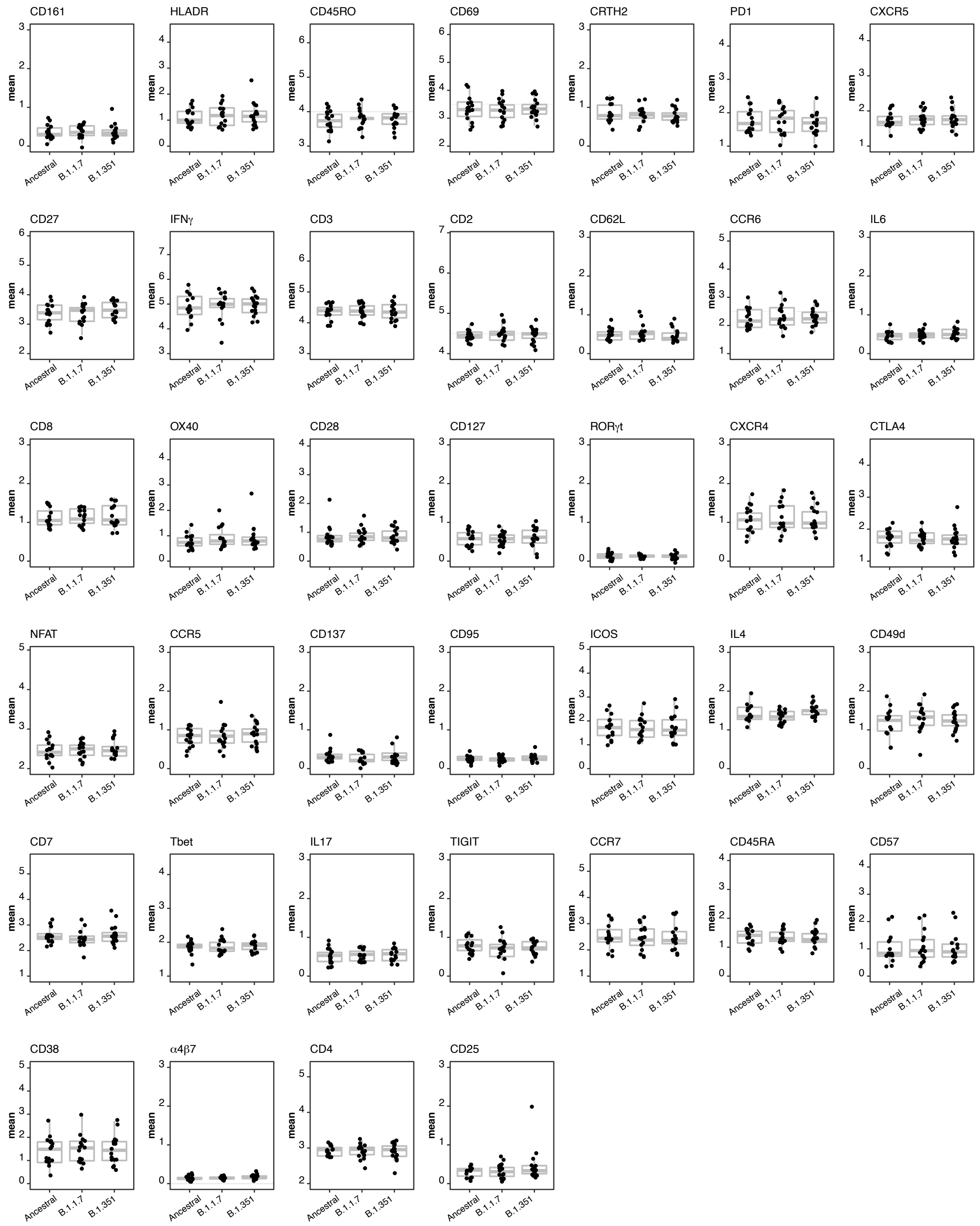
CD161
HLADR
CD45RO
CD69
CRTH2
PD1
CXCR5
CD27
IFNγ
CD3
CD2
CD62L
CCR6
IL6
CD8
OX40
CD28
CD127
RORγt
CXCR4
CTLA4
NFAT
CCR5
CD137
CD95
ICOS
IL4
CD49d
CD7
Tbet
IL17
TIGIT
CCR7
CD45RA
CD57
CD38
α4β7
CD4
CD25
mean
Ancestral
B.1.1.7
B.1.351

Figure S3

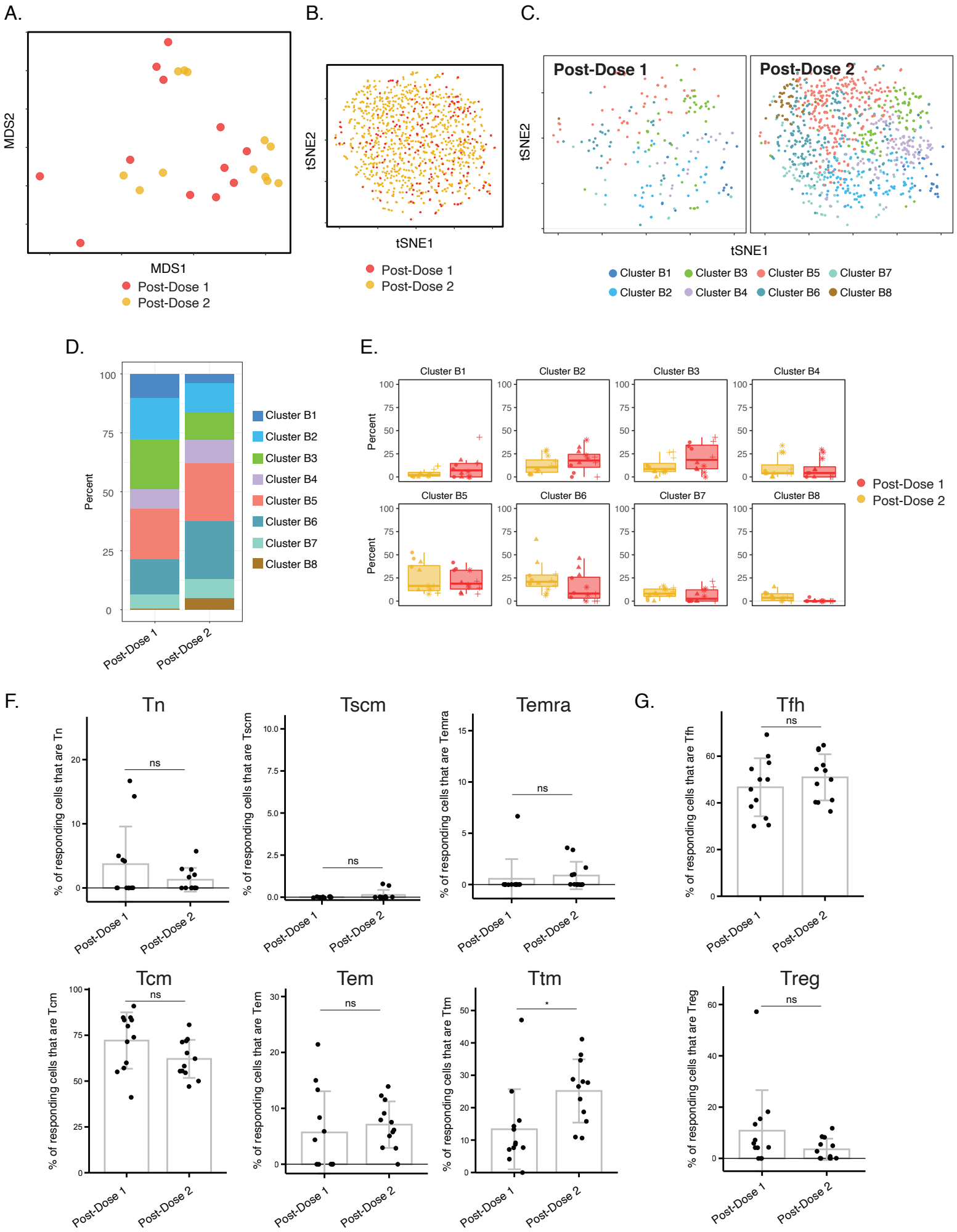
A.
MDS2
MDS1
Post-Dose 1
Post-Dose 2
B.
tSNE2
tSNE1
Post-Dose 1
Post-Dose 2
C.
Post-Dose 1
Post-Dose 2
tSNE2
tSNE1
Cluster B1
Cluster B2
Cluster B3
Cluster B4
Cluster B5
Cluster B6
Cluster B7
Cluster B8
D.
Percent
Post-Dose 1
Post-Dose 2
E.
Cluster B1
Cluster B2
Cluster B3
Cluster B4
Cluster B5
Cluster B6
Cluster B7
Cluster B8
Percent
Post-Dose 1
Post-Dose 2
F.
Tn
Tscm
Temra
G.
Tfh
Tcm
Tem
Ttm
Treg
% of responding cells that are Tn
% of responding cells that are Tscm
% of responding cells that are Temra
% of responding cells that are Tfh
% of responding cells that are Tcm
% of responding cells that are Tem
% of responding cells that are Ttm
% of responding cells that are Treg
ns
*
Post-Dose 1
Post-Dose 2

Figure S4

A.

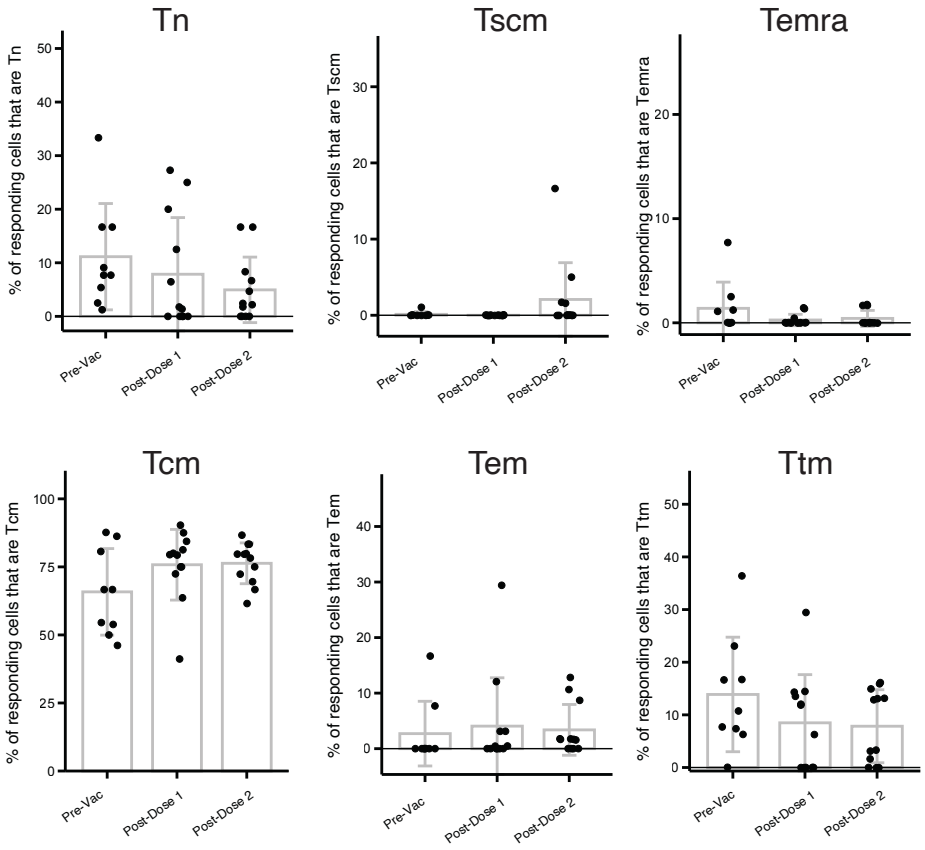
Tn
% of responding cells that are Tn
Tscm
% of responding cells that are Tscm
Temra
% of responding cells that are Temra
Tcm
% of responding cells that are Tcm
Tem
% of responding cells that are Tem
Ttm
% of responding cells that are Ttm
Pre-Vac
Post-Dose 1
Post-Dose 2

B.

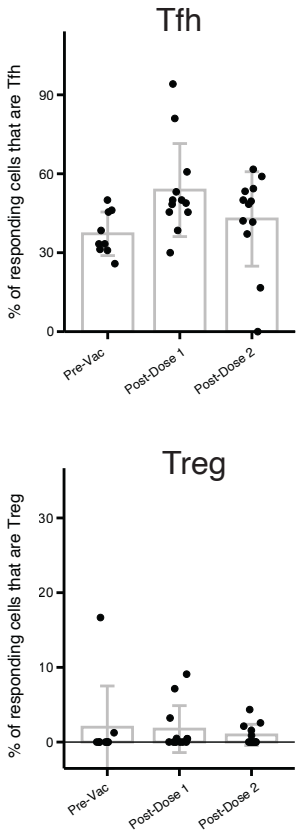
Tfh
% of responding cells that are Tfh
Treg
% of responding cells that are Treg
Pre-Vac
Post-Dose 1
Post-Dose 2

Figure S5

A.

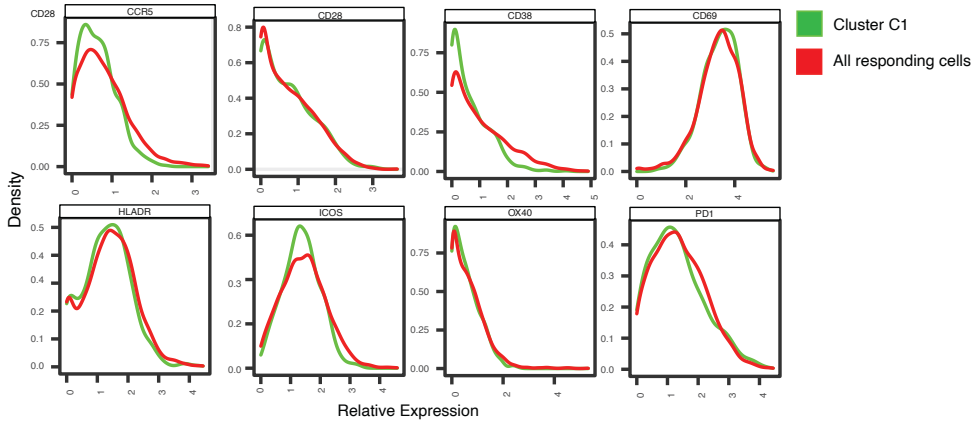
CCR5
CD28
CD38
CD69
HLADR
ICOS
OX40
PD1
Density
Relative Expression
Cluster C1
All responding cells

B.

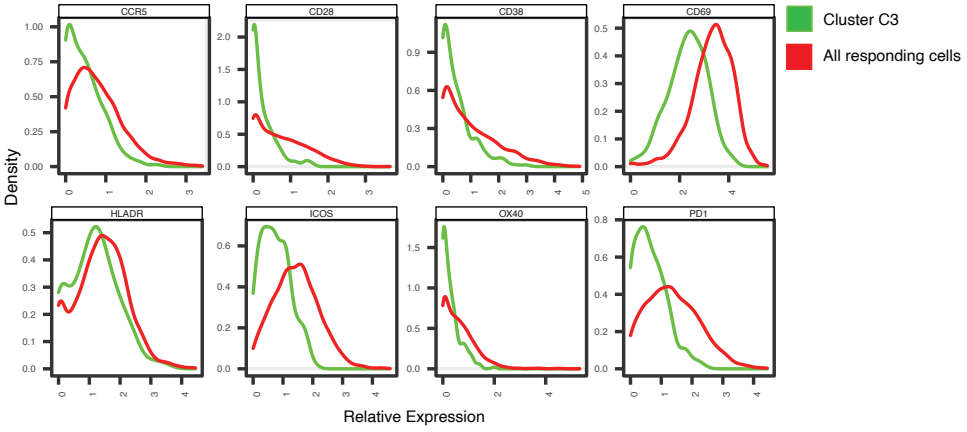
CCR5
CD28
CD38
CD69
HLADR
ICOS
OX40
PD1
Density
Relative Expression
Cluster C3
All responding cells

Figure S6

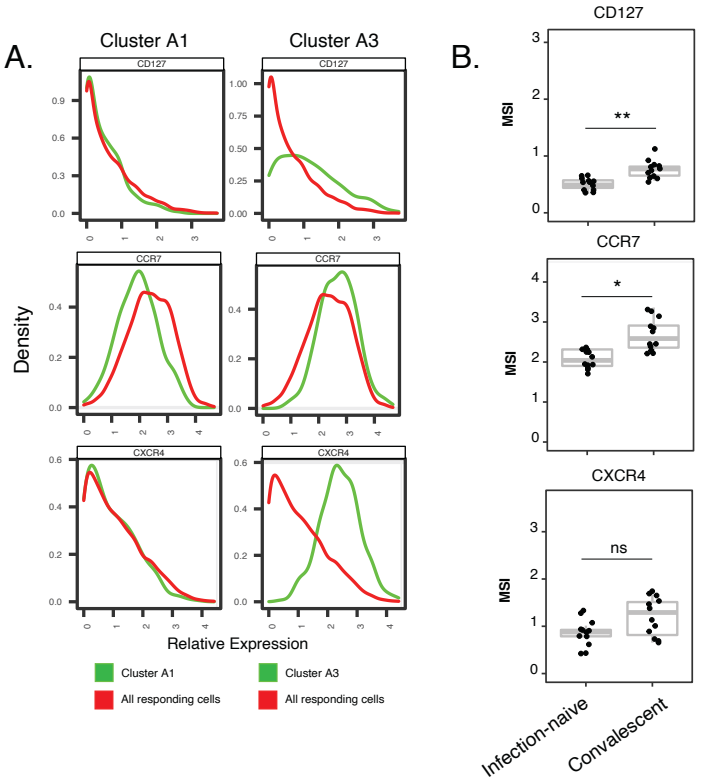
A.
Cluster A1
Cluster A3
CD127
CCR7
CXCR4
Density
Relative Expression
Cluster A1
All responding cells
Cluster A3
All responding cells
B.
CD127
CCR7
CXCR4
MSI
**
*
ns
Infection-naive
Convalescent

Figure S7

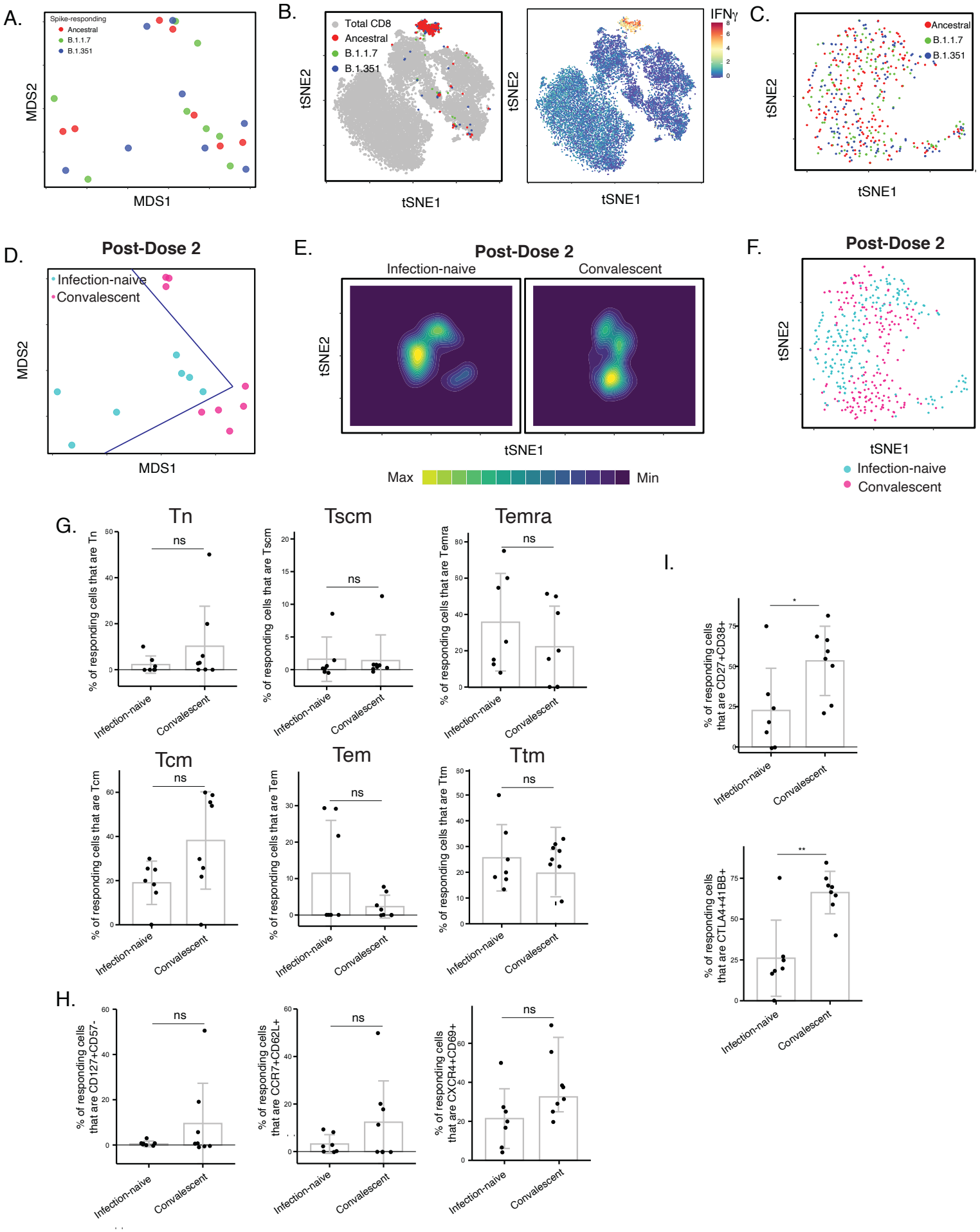
A.
Spike-responding
Ancestral
B.1.1.7
B.1.351
MDS2
MDS1
B.
Total CD8
Ancestral
B.1.1.7
B.1.351
tSNE2
tSNE1
IFNγ
C.
Ancestral
B.1.1.7
B.1.351
tSNE2
tSNE1
D.
Post-Dose 2
Infection-naive
Convalescent
MDS2
MDS1
E.
Post-Dose 2
Infection-naive
Convalescent
tSNE2
tSNE1
Max
Min
F.
Post-Dose 2
tSNE2
tSNE1
Infection-naive
Convalescent
G.
Tn
Tscm
Temra
Tcm
Tem
Ttm
ns
% of responding cells that are Tn
% of responding cells that are Tscm
% of responding cells that are Temra
% of responding cells that are Tcm
% of responding cells that are Tem
% of responding cells that are Ttm
Infection-naive
Convalescent
I.
*
**
% of responding cells that are CD27+CD38+
% of responding cells that are CTLA4++41BB+
H.
% of responding cells that are CD127+CD57-
% of responding cells that are CCR7+CD62L+
% of responding cells that are CXCR4+CD69+